NON-FLUORINE PRECURSOR SOLUTIONS FOR HIGH CRITICAL CURRENT DENSITY $REBa_2Cu_3O_{7-x}$ FILMS

By

Yoda Rante Patta

S.T.
Institut Teknologi Bandung, 2004

Submitted to the Department of Materials Science and Engineering
in Partial Fulfillment of the Requirements for the Degree of

Master of Science in Materials Science and Engineering
at the
Massachusetts Institute of Technology

June 2008

Signature of Author ……...
Yoda Rante Patta
Dept. of Materials Science and Engineering
April 23, 2008

Certified by ……...
Michael J. Cima
Sumitomo Electric Industries Professor of Engineering
Thesis Supervisor

Accepted by ..……...
Samuel M. Allen
POSCO Professor of Physical Metallurgy
Chair, Departmental Committee on Graduate Students

Non-Fluorine Precursor Solutions for High Critical Current Density $REBa_2Cu_3O_{7-x}$ Films

By

Yoda Rante Patta

Submitted to the Department of Materials Science and Engineering
in Partial Fulfillment of the Requirements for the Degree of
Master of Science in Materials Science and Engineering
at the Massachusetts Institute of Technology

ABSTRACT

The past two decades have seen advancements in high temperature superconducting cables for use in applications such as electrical transmission lines, propulsion systems, and mobile power generation systems. This work describes the development of a non-fluorine precursor solution for YBCO films with high critical current densities (J_c). An aqueous nitrate precursor solution system was selected from three possible precursor solution systems. It was further developed to produce YBCO films with $J_c > 1$ MA/cm^2. Films up to ~800 nm thickness were made, and $J_c > 1$ MA/cm^2 was obtained for films of over ~400 nm thickness. The developed aqueous solution contained a rheology modifier (hydroxyethyl cellulose / HEC), nitrates of Y, Ba, and Cu, and chelating agents (polyethylene glycol / PEG and sucrose). The total organic content was ~12 wt% of the entire solution, and the total cation concentration was ~0.7 M. The rheology modifying polymer determined the thickness of the deposited films. This allowed for the deposition of films with higher thickness than would be dictated by the total dissolved cations alone.

A low temperature decomposition process was developed based on analyses of the chemical reactions that take place in the precursor films as they were heated. This process produced smooth and defect-free intermediate films that were stable under ambient conditions. These films were then heat treated to convert them into YBCO films. Recommendations for future work include further improvements to the precursor solution, including more effective chelating agents and possible alternative solvent systems. Intermediate films thicker than 2.5 μm still tended to have surface defects. Additional in-depth thermal analysis would further show how these defects develop, and adjustments to the decomposition process could be made accordingly. High resolution plan-view and cross-sectional microstructures of the films between the precursor state and their converted forms is recommended. These future studies will be valuable in further improving the performance and thickness of films derived from the non-fluorine precursor solution developed in this thesis.

Thesis Supervisor: Michael J. Cima
Title: Sumitomo Electric Industries Professor of Engineering

TABLE OF CONTENTS

LIST OF TABLES AND FIGURES

ACKNOWLEDGMENTS

These pages summarize the result of several years' worth of experiments done in the basement of MIT's building 12. This time has been challenging, and I've learned so much more than I ever expected to. I am grateful to the following parties, without whom this work would not be possible.

To Michael Cima, my advisor, for all of his support, insight, and guidance, and for challenging all of us to become better researchers. Being part of his group has made, and continues to make, my graduate school experience especially memorable, and for that I am thankful.

To Dan Wesolowski, my lab partner, my mentor, and my best friend. It's impossible to list all the things that I've learned from him these past few years, but suffice it to say that I can't imagine what the past three years would have been like without him.

To the people at CPRL: Lenny, whose help and knowledge in the many analytical techniques are invaluable. Barbara, whose organization and support make the daily details of research much smoother. My fellow Cima Lab group-mates Grace, Chris, Hong Linh, Heejin, Karen, Irene, Yibo, Noel, Alex, and Byron, for all the discussions, advice and encouragement. One of my favorite things about being in this group is the people—the fact that we're all friends makes work that much more enjoyable and interesting.

To Sumitomo Electric Industries, for funding this project and for providing great feedback and discussion during the course of this work.

To Scott Speakman, Tim McClure, Judy Maro, Steve Kooi, and Libby Shaw, for their help in using the different analytical techniques that were a crucial part of this work.

To my family, who love me unconditionally, and whose love I continue to feel everyday in my life even though we are half a globe apart.

To my friends, who keep me sane and continue to remind me of how good life is.

To MIT, this strange and wonderful place that has challenged and pushed me beyond the point where I thought I could go, and allowed me to discover strengths I never knew I had.

CHAPTER 1: BACKGROUND AND MOTIVATION

1.1 High Temperature Superconductors

The discovery of high temperature superconductors in the 1980s has spurred widespread interest and research in the processing, properties, and performance of superconducting wires for a variety of applications [12]. High temperature superconductors (HTS) could be used in applications where high current densities and high magnetic fields are required. Cables containing HTS with orders of magnitude higher current densities could replace conventional copper cables in electrical transmission lines in power grids. The high current densities and lower weights of superconducting cables can be used in motors and transformers in propulsion systems and mobile power generation systems [56,2]. The potential applications of superconducting wires are extensive, and the benefits that they would bring are motivation for further research to achieve the highest performances possible through materials selection and processing.

There are two different architectures for HTS cables. The first generation (1G) superconductor architecture takes the form of fine filaments of $Bi_2Sr_2Ca_2Cu_3O_{10}$ (BSCCO-2223) in a matrix of silver or silver alloy. Second generation (2G), or coated conductor, architecture consists of textured metal substrates coated with buffer layers and an epitaxial superconducting layer. The superconducting layer is $REBa_2Cu_3O_{7-x}$, where RE is a rare earth metal such as yttrium or holmium. This thesis work is focused on $YBa_2Cu_3O_{7-x}$ (YBCO), which has a superconducting transition temperature (T_c) of 93K [28,7].

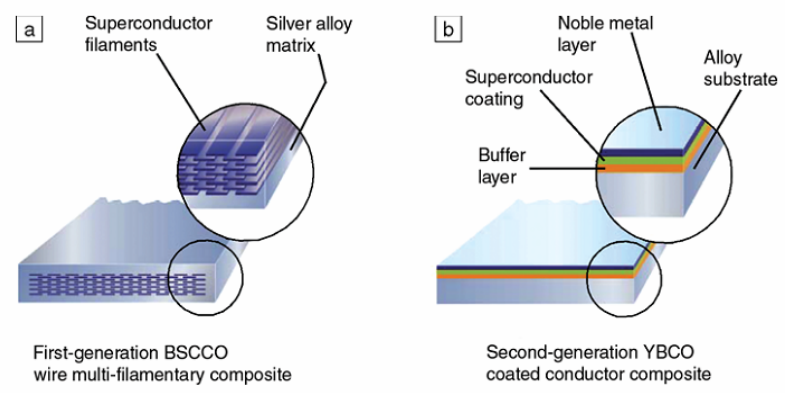

Figure 1. Architectures for HTS wires [2]

1.2 YBCO Microstructure and Current-Carrying Performance

The microstructure of a YBCO film strongly affects its critical current density (J_c), critical current (I_c), transition temperature (T_c), and in-field J_c [8]. Current flow in a polycrystalline superconducting layer is made very difficult by the presence of large angle grain boundaries [910,11,12]. Dimos et al found that J_c across a grain boundary on the a-b plane is less than that within the bulk, with the disparity becoming worse with higher angles [14]. Misorientation angles beyond 2º have been found to result in an exponential decrease of J_c across the grain boundaries in YBCO films [12,1].

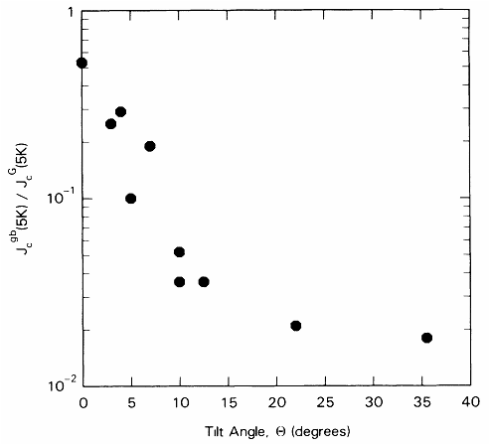

Figure 2. Ratio of J_c across a grain boundary over bulk J_c vs. grain misorientation angle [13]

The importance of microstructure in the performance of YBCO films is evident in measurements of J_c vs. film thickness for thick (>500 μm) YBCO films. A rapid drop-off in J_c is observed between the YBCO near the interface with the substrate and the YBCO that makes up the rest of the film. A high density of flux-pinning misfit dislocations near the substrate-YBCO interface, as observed in TEM, may explain this trend in J_c vs. thickness [16].

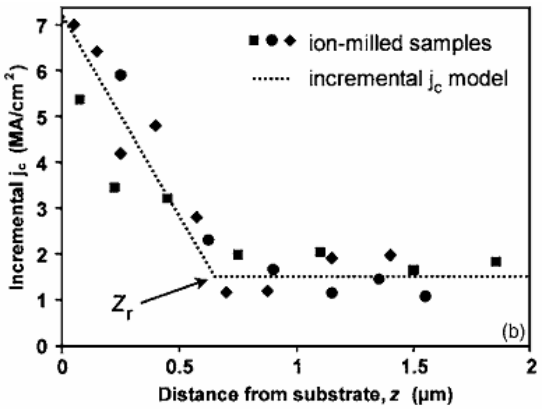

Figure 3. Experimental data (with overlaid model) showing J_c vs. thickness [16]

1.3 Deposition Processes

YBCO coated conductors are deposited by a variety of techniques. Physical deposition processes include pulsed laser deposition (PLD) and e-beam deposition. Chemical deposition techniques include chemical vapor deposition (CVD), metalorganic chemical vapor deposition (MOCVD), sol-gel, spray pyrolysis, metalorganic deposition (MOD), and electrodeposition. These techniques are used either to deposit YBCO directly on a substrate (*in situ*), or deposit the cations in other forms, as salts or oxides, to be converted through heat treatment into the final YBCO layer (*ex situ*) [8]. Both types of techniques produce high performance YBCO films with critical current densities of several MA/cm^2 [2]. YBCO films are deposited on textured buffered

layers that serve as a template for growth of a film with the desired grain orientation (00l). The microstructure of *in situ* films such as those grown by PLD is columnar. *Ex situ* films such as those grown by MOD have a laminar, layered microstructure [2,17].

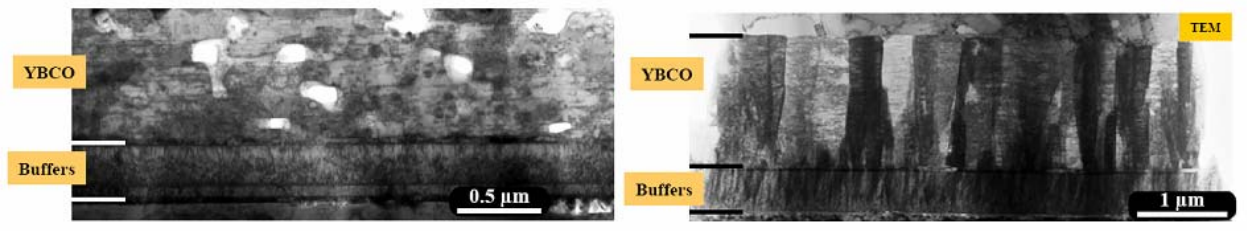

Figure 4. Microstructures of MOD (laminar, left) and PLD (columnar, right) YBCO films

1.4 Solution Deposition Processes

There are several advantages to choosing solution deposition as the processing technique for depositing YBCO precursor films. The stoichiometry of the film can be easily controlled by tailoring the chemistry of the precursor solution [18]. Multiple layers of coating can be deposited to increase the total film thickness [1916,20]. There are also added processing flexibilities for depositing films over larger areas and/or longer substrate lengths [21].

The current state-of-the-art solution deposition process for producing YBCO films is the TFA (trifluoroacetate) MOD process. Work done by various groups has produced TFA-MOD films with critical current densities exceeding 10 MA/cm^2 and critical currents above 700 A/cm-width [2]. Work done at MIT has reliably produced high critical current density (>1 MA/cm^2) near-micron thick YBCO films using the TFA-MOD process [22].

The presence of fluorine in the precursor results in formation of BaF_2, which is more stable than $BaCO_3$ [23]. Work done by Shaw et al shows that carbon in YBCO films is usually present in the form of barium carbonate. Incomplete decomposition of $BaCO_3$ and the resulting incomplete removal of carbon is a source of contamination in the final YBCO films [2425].

Carbon contents between 0.5-1.2 wt% results in lowering of T_c to ~50 K in close-porosity films from which removal of carbon is more difficult [25]. This is an important aspect of the processing of YBCO films that are made from organic-containing, non-fluorine precursor solutions.

The TFA process still has its disadvantages. Reaction between the fluoride compounds and flowing water vapor in the atmosphere during heat treatment results in evolution of HF gas. The removal of HF gas from the system limits growth of the YBCO. Complex reactor designs that maintain uniform gas flow and P(HF) across the sample are thus necessary to produce uniform films [26,19]. This complication limits the width of YBCO that can be uniformly processed. Additionally, the reactions that must take place during the conversion of the precursor film to the final film result in long processing times. The TFA process developed at MIT, for instance, involves an overnight decomposition step prior to the high temperature conversion step. These disadvantages provide motivation to develop solution deposition processes for superconducting YBCO films from non-fluorine containing precursors, despite the possible $BaCO_3$ challenges.

1.5 Organization of Thesis

The ultimate aim of this thesis work is to develop a non-fluorine precursor solution for deposition of high critical current density YBCO films. Within this scope there are several specific aims, each of which will be discussed in the following chapters. Chapter 2 will cover the selection of one out of three non-fluorine solution deposition processes based on a set of pre-determined criteria. Chapter 3 will encompass the work done to further develop that process to improve film characteristics and increase performance (J_c) and film thickness. Chapter 4 will

include a discussion of the chemical reactions taking place in the film as it undergoes heat treatment and the development of a low temperature heat treatment to obtain a high quality intermediate or decomposed precursor film. Chapter 5 will conclude with a summary of the work done and recommendations for future work.

CHAPTER 2: SELECTION OF NON-FLUORINE SOLUTION DEPOSITION SYSTEM

2.1 Introduction

The literature on non-fluorine solution deposition processes reveals a variety of non-fluorine systems that have been researched to produce superconducting thin films. Work has been done by different groups on non-fluorine systems comprising of acetylacetonates, trimethylacetates, naphthenates, alkoxides, and nitrates of the cations that make up the superconductor [27,28,30,21,31,32]. The outcomes of these processes vary, with films of less than 100 nm to more than 1 μm in thickness, and from no J_c values reported to J_c values of a few MA/cm^2. Likewise, the processes differ in their degree of complexity, processing time, amount and toxicity of reagents, and other factors that affect how straightforward it would be to obtain films of a certain thickness with a particular performance threshold.

A number of non-fluorine based processes have demonstrated high performance (>1 MA/cm^2) YBCO films. Kumagai and co-workers have produced ~200 nm films with J_c values in excess of 4 MA/cm^2 on single crystal substrates. Their precursor solution consists of Y, Ba, and Cu acetylacetonates [19]. Researchers at Oakridge National Labs (ORNL) have developed a $Ba(OH)_2$ and Y and Cu trimethylacetate (TMA) based route which also has produced thin (~100nm) films of >1 MA/cm^2. The acetylacetonates are dissolved in a mixture of pyridine and propionic acid solvent [30,32,33]. Lu and co-workers at the University of Wisconsin produced 0.9 μm (Y,Sm)BCO films on rolling assisted biaxially textured (RABiTS) substrates with J_c up to 1.7 MA/cm^2.

These non-fluorine MOD routes have apparently solved the $BaCO_3$ formation problem, but have some drawbacks. The precursor components are toxic and/or dangerous. Solution preparation schemes can be complex, often requiring multiple drying and re-dissolving steps to

obtain the final chemicals that go in the solution. Film layer thicknesses per deposition are quite thin because of the poor solubility of Ba. The acetylacetonate process, for instance, required fifteen coatings to obtain the desired thickness [20]. The conversion heat treatment can be quite complex and, in the case of the TMA process, requires high water vapor pressure, which complicates reactor design.

Researchers at Wright State University have developed a colloidal YBCO solution deposition technique. A colloid suspension containing oxide nanoparticles with particle sizes of about 10 nm is deposited by spin coating and heat treated to 750ºC. The advantage in being able to use the colloidal suspension is that the precursors start in the form of oxides, which would reduce processing times. YBCO films produced with the nano-colloidal process had a T_c of 80.2 K. No critical current values were reported [34].

Several researchers have turned to metal-nitrate solutions to create simpler and safer non-fluorine based deposition techniques. Low toxicity and low cost solvents such as water and methanol are generally compatible with nitrates. However, nitrate solutions may pose several challenges for film production. Some of these challenges are the hydroscopic nature of the reagents, the necessity of decomposing nitrates during heat treatment, and difficulty in getting the solution to wet the oxide or oxide-coated metal substrate [35].

One solution to the substrate wetting problem is to spray the nitrate solution onto a heated substrate. Gupta et. al. have obtained ~1-3 micron YBCO films on YSZ substrates with J_c = 42 A/cm^2 at 77 K using a process in which an all-nitrate solution is sprayed onto a heated (~180^{o}C) substrate and subsequently heated to ~900-950^{o}C under flowing oxygen [31]. This process has been refined by Supardi et al. They have produced ~2 micron films with J_c ~ 1.4 MA/cm^2 at 77

K by spraying an all-nitrate solution onto heated (~850°C) single-crystal STO substrates, followed by annealing at that temperature for 120 minutes [37].

Apetrii et al have produced 250 nm YBCO films on single crystal $SrTiO_3$ (STO) substrates with J_c values of 1 MA/cm^2 at 77 K using a polyacrylic acid-nitrate precursor solution in dimethylformamide. Their films are first heated at 170°C for 3 hours before going through high-temperature annealing at 775°C [21]. A number of other reports have fabricated other metal oxide films from nitrate-based solutions [38,39,40]. These authors have all chosen to use organic solvents as the solution vehicle. Polymer solubility and substrate wetting are improved while solubility of the cations is maintained. Jia et al have reported on polymer-assisted deposition of films, including those incorporating aqueous solutions of nitrates, polyethyleneimine (PEI), and ethylenediamine tetraacetic acid (EDTA). This work has produced crystalline YBCO, but no critical current densities have been reported [41].

Table 1. Selected summary of work done on non-fluorine systems by other groups

Author	Year	Location	Deposition Method	Ligand	Solvent	Thickness (nm)	J_c, 0T, 77K (A/cm^2)
Rice [42]	1987	AT&T Bell Labs	Spin/dip coating	Acetate	Acetic acid/water	160	(T_c=58 K)
Hamdi [27]	1987	GM Research Labs	Spin coating	Neodecanoate	Xylene/pyridine	500	(T_c=17 K)
Kumagai [28]	1987	AIST (Japan)	Dip coating	Ba, Cu-naphthenates, Y-stearate	Toluene		(T_c=60 K)
Kordas, G. [43]	1990	Univ. of Illinois	Spin coating	Cu-ethoxide, Ba, Y-methoxyethoxide	Toluene, methoxyethanol	1000	
Bowmer, T. and Shokoohi, F.[44]	1990	Bellcore	Spin/dip coating	Neodecanoate	Xylene/ 5% pyridine or toluene/ 5 % pyridine		50
Manabe [19]	1991	AIST (Japan)	Spin coating	Acetylacetonate	Propionic acid/Pyridine (and methanol)	2000	0.39 x 10^6

Kumagai [28]	1992	AIST (Japan)	Spin coating	Naphthenates	Toluene	1000	1.1 x 10^6
Chu [45]	1993	Univ. of Illinois	Spin coating	Trimethylacetate	Propionic acid/amylamine and xylene		0.13 x 10^6
Rupich [46]	1993	EIC Laboratories	Spin coating	Alkoxides	Pyridine, also 2-methoxyethanol		0.2 x 10^6
Kumagai [28]	2001	AIST (Japan)	Dip coating	Acetylacetonate	Propionic acid/Pyridine (and methanol)	400	1 x 10^6
Supardi [37]	2002	LMGP-INGP, France	Spray pyrolysis	Nitrate	Water	1000	1.4 x 10^6
Xu [32]	2003	ORNL	Spin coating	Y, Cu-trimethylacetate and barium hydroxide	Propionic acid/amylamine and xylene	70-100	1.65 x 10^6
Shi [30]	2004	University of Cincinnati	Spin coating	Y, Cu-trimethylacetate and barium hydroxide	Propionic acid/amylamine and xylene	500	0.1 x 10^6
Apertrii [21]	2005	Leibniz Inst (Germany)	Spin coating	Polyacrylic, nitrates	Dimethylformamide	250	1.0 x 10^6
Tsukada [19]	2005	AIST (Japan)	Spin coating	Acetylacetonate	Propionic acid/Pyridine (and methanol)	200	4.0 x 10^6
Lu [20]	2006	University of Wisconsin	Spin coating	Acetylacetonate	Propionic acid/Pyridine (and methanol)	900	1.7 x 10^6

2.2 Selection of Non-Fluorine Solution Deposition Process

The first specific aim of this thesis work is to produce YBCO films by three different non-fluorine solution deposition systems and select one that has the most promise. The main criteria for selection of the overall process are (1) critical current density > 1 MA/cm^2, (2) thickness that can exceed 500 nm, and (3) the potential for further improvements to increase J_c and thickness. Bhuiyan et al have outlined criteria for a precursor solution that will produce quality superconductors [18]. These criteria are as follows.

(1) The solution is stable, with sufficient solubility.

(2) The cations remain in the film during/after heat treatment, but all decomposed ingredients are released into the flowing gas stream with no film residues remaining.

(3) Crystallization or macroscopic phase separation of the individual precursor components upon evaporation of the solvent are prevented.

(4) The solution wets the substrate and produces an overall deposited layer.

(5) The rheology and flow of solution can be adjusted to obtain the desired film thickness.

(6) Lack of cracking or compositional non-uniformities during heat treatment.

(7) Interdiffusion between the film and substrate is minimized.

(8) Degradation of substrate properties is minimized.

(9) Long term stability of the solution is possible; solution ageing is minimized.

These criteria were used as guidelines for selecting one of the three processes to be further developed as a high-J_c non-fluorine solution deposition process.

Three different precursor solutions were examined in this part of the thesis: a trimethylacetate-based solution, a particulate-alkoxide solution, and an aqueous polymer-nitrate solution. Each solution was spin-coated onto single crystal (100) lanthanum aluminate (LAO) substrates using a photoresist spinner. The resultant precursor film was heat treated under a low oxygen atmosphere (approximately 100 ppm O_2/N_2) to annealing temperatures between 740ºC and 760ºC. Some variations to the heat treatment were applied depending on the process, including the use of water vapor and/or other oxygen partial pressures. Critical currents of the films were measured under 77 K and self-field using a four-point probe type measurement.

Optical and SEM micrographs were taken of films from each process. High resolution micrographs were taken using a Hitachi S-530 or a JEOL JSM-6060 SEM under secondary

electron mode. XRD patterns were obtained using a Rigaku R-200 three-circle diffractometer with a rotating anode source at 50 kV and 300 mA. Film thicknesses were measured by using the Tencor P10 Profilometer. Composition of the precursor solutions and dissolved films were measured by using the Spectro Ciros Vision inductively coupled plasma (ICP) atomic emission spectroscopy. Measurements of the relative carbon content in the film was done by wavelength dispersive spectroscopy (WDS) using a JEOL JXA-733 Electron Probe Microanalyzer (EPMA) at 15 kV accelerating voltage and 10 nA current. The relative elemental composition of the film surface was obtained using a PHI 700 Scanning Auger Nanoprobe at 10 kV accelerating voltage.

2.3 Trimethylacetate-Based Precursor Solution

2.3.1 Experimental Procedure

2.3.1.1 Precursor Solution Preparation

Work by Shi et al was used as a starting reference for the experimental procedures and as a comparison for the resulting films [30,32,33]. Yttrium acetate ($Y(CH_3COO)_3$) and copper nitrate ($Cu(CH_3COO)_2$) were separately dissolved in water. A separate solution of ammonium trimethylacetate ($NH_4(C_4H_9COO)$) was made by reacting trimethylacetic acid (C_4H_9COOH) and 10-30% excess ammonium hydroxide (NH_4OH). The aqueous acetate solutions were mixed with ammonium trimethylacetate. Light blue-green copper trimethylacetate (which will be referred to as $Cu(TMA)_2$) powder and white yttrium trimethylacetate ($Y(TMA)_3$) precipitates were then formed from the solution. After mixing for at least thirty minutes to ensure that enough trimethylacetates were formed, the remaining solution was filtered away from the wet precipitate powders. This process was repeated several times. The wet powders were washed again with the ammonium hydroxide – trimethylacetic acid solution to ensure that all of the remaining

precipitates were fully converted to $Y(TMA)_3$ and $Cu(TMA)_2$. These cakes were then dried inside a vacuum furnace overnight. $Y(TMA)_3$, $Ba(OH)_2$, and $Cu(TMA)_2$ were added together in a nominal stoichiometric ratio of Y: Ba: Cu = 1: 1.8: 3 and dissolved in a 4:3 propionic acid: amylamine (n-pentylamine) solvent to make a dark blue precursor solution. The total cation concentration of the solution was between 0.5 and 0.6 M, with an ICP measured stoichiometry of 1: 1.83: 3.01.

2.3.1.2 Deposition and Heat Treatment

The trimethylacetate (TMA) precursor solution was deposited on LAO substrates at a rate of 4000 rpm for 30 seconds. The substrate was then placed on a hot plate at a temperature between 110ºC and 120ºC to prevent dewetting of the film from the substrate. Higher thicknesses may be obtained by spin-coating additional layers on top of a first layer that had been heated on the hot plate.

The precursor film was heat treated in a tube furnace with wet O_2 gas (bubbler water dew point ~40ºC) through a decomposition step at 400ºC, followed by a high temperature (variable $T_{conversion}$ = 730-800ºC) conversion step under flowing wet 100 ppm O_2/N_2 gas. The film was then cooled under dry 100 ppm O_2/N_2 gas, followed by an oxygen annealing step at 525ºC before furnace cooling to room temperature under dry O_2.

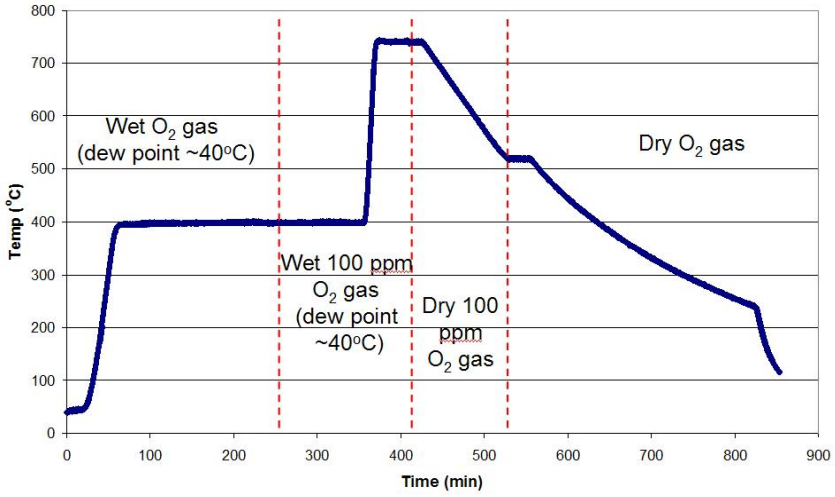

Figure 5. Heat treatment profile for TMA process

2.3.2 Results and Discussion

The spin-coated TMA films were very smooth, but the film's adherence to the substrate was limited, thus the need for a drying step immediately following spin coating. The low concentration of cations in the precursor solution and lack of polymers in solution to assist in wetting of the substrate resulted in thin films of less than 100 nm per layer. Multiple coating increases the thickness of the overall film, but only by so much. Four layers made up a ~250 nm final film, but nine layers also made up that same thickness. It was likely that subsequent spin-coating of layers resulted in dissolution of the layer(s) already deposited, reducing the total amount of material that actually remains on the substrate. It was found that adding more than four coats did not serve to increase the thickness of the final film.

A θ-2θ scan of a representative TMA film showed a highly c-axis oriented YBCO film. Pole figure and micrographs at low and high magnification showed the epitactic structure of the TMA films.

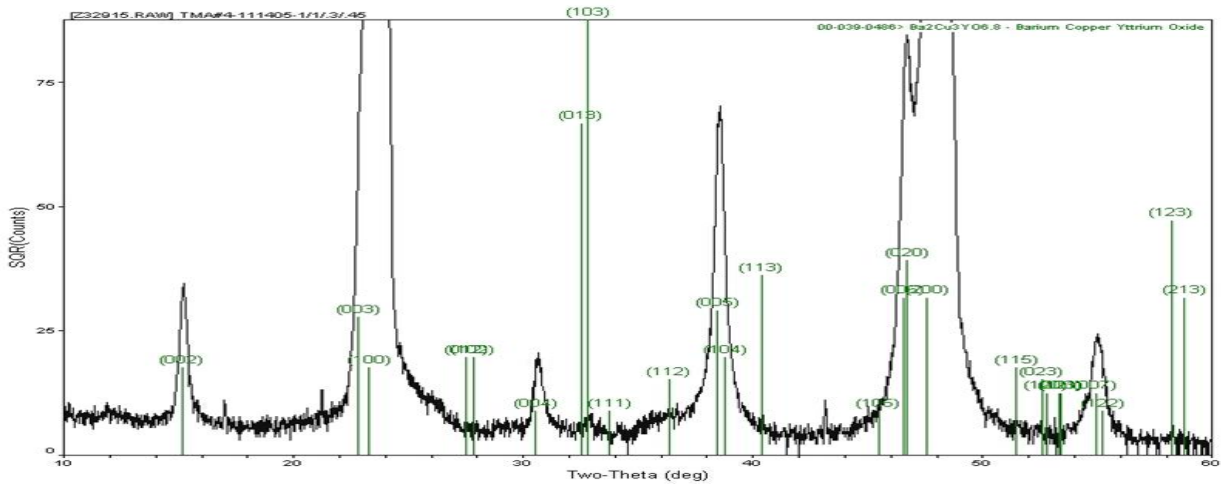

Figure 6. c-axis textured YBCO film from TMA precursor

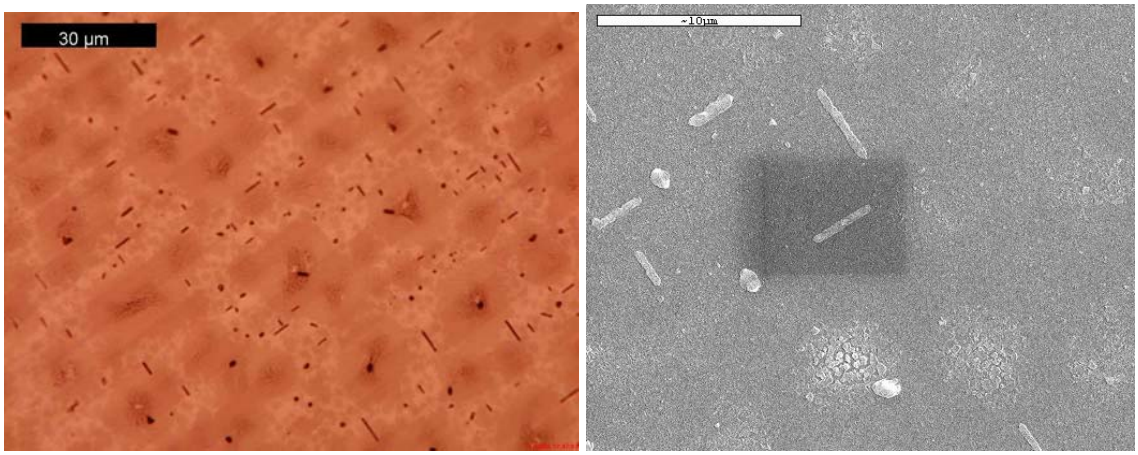

Figure 7. Optical and SEM micrographs of TMA films showing large a-axis grains

Despite evidence of epitaxial YBCO, none of the TMA films produced carried current at 77 K under self field. The room temperature resistance values for TMA films were quite high, ranging from 700 Ω to more than 3000 Ω. The room temperature resistances of MA/cm^2 TFA films usually fall below 40 Ω. Room temperature resistances were used as a fast indicator of whether or not a film would become superconducting and carry current at 77 K.

Although the TMA process had been shown to work elsewhere, there were several difficulties in reproducing those results. There may have been excess acetates in the precursor solution from incomplete reactions to form the trimethylacetate compounds. The powders were washed several times, but there may still be acetates left even after those steps. The low solution concentration and difficulty of wetting the substrate made obtaining a sufficiently thick film that coats the entire substrate quite complicated. Even multiple coatings could not significantly build the thickness. The conversion process to achieve the final YBCO film required high water vapor partial pressures. This in turn required a complex furnace set-up to prevent condensation of water vapor in the tube that carried the gas stream to the interior of the furnace. These difficulties suggested that if another precursor solution route could be taken that produced thicker films, better wet the substrate, and did not involve an intermediate chemical preparation step, that route would be preferable to the TMA precursor solution route.

2.4 Alkoxide-Based Precursor Solution

The second solution deposition route tested incorporated alkoxides of yttrium and barium and copper oxide particles. The hydrolysis of metal alkoxides is often used in sol-gel processes, but in this particular process any gelling of the separate alkoxides was prevented until all of the cations were deposited together on the substrate. Furthermore, a granular or colloid precursor system, such as one used by Mukhopadhyay et al at Wright State University, had been suggested to produce films with lower porosity at a faster rate (the state of the precursor film would be closer to the final film) [34].

2.4.1 Experimental Procedure

2.4.1.1 Precursor Solution Preparation

As-received barium 2-methoxyethoxide ($Ba(OCH_2CH_2OCH_3)_2$, or $Ba(2\text{-}ME)_2$ in short) and yttrium 2-methoxyethoxide were analyzed by ICP to determine the actual cation concentration. It was found that there was a 20-30% difference between the as-received label and the actual cation content. Using this information, corrected amounts of the as-received alkoxides, in a nominal ratio of Y: Ba: Cu = 1: 2: 3, were dissolved in 2-methoxyethanol. The solution was then distilled to increase the Y cation concentration from ~0.083 M to ~0.131 M. Effort was made to keep the alkoxide solution from being exposed to ambient atmosphere by doing most of the mixing inside a nitrogen atmosphere glove box. No hydrolysis of the alkoxides into gels was observed with this procedure.

A separate suspension of as-received CuO nanoparticles in 2-methoxyethanol was prepared. A proportionate weight of CuO needed to complete a 1:2:3 stoichiometric ratio was suspended in 2-methoxyethanol solvent. The CuO nanopowder, with a stated average particle size of 33 nm, was agglomerated and aggregated into sizes larger than 0.1 μm. Steps to break up the aggregates and agglomerates, and keeping the particles apart, were undertaken. CuO in 2-methoxyethanol suspensions were milled, ultrasonicated, or both, and the resulting particle size distributions measured. Milling was done using a vibratory mill with zirconia milling media in an HDPE bottle. Particle size distributions were obtained using a Horiba Particle Size Distribution Analyzer (CAPA-700).

Several different commercial nonionic dispersants were subsequently tested for their effectiveness in keeping the broken up CuO agglomerates and particles dispersed in the solvent. A combination of these steps and the best choice for dispersant (polyethyleneimine (PEI), as will

be discussed below) were used to obtain the CuO suspension in 2-methoxyethanol to be combined with the Y and Ba alkoxides from the previous step. Further improvement to the solution preparation combined the two segments into one. Distillation of the Y and Ba alkoxides was followed by addition of the PEI and CuO nanopowder. The entire mix was then ultrasonicated to obtain the final precursor solution. This precursor had a final dissolved cation concentration of ~0.39 M, with an ICP measured stoichiometry of Y: Ba: Cu = 1: 2.07: 3.02.

2.4.1.2 Deposition and Heat Treatment

The alkoxide suspension precursor was deposited on LAO substrates at a rate of 3000-4000 rpm for 30-60 seconds. No drying step was required; the films adhered on the surface of the substrate without heating on a hot plate. Multiple coatings, however, do require a drying step on a hot plate between layers to prevent significant dissolution of the layer(s) already deposited. The precursor film was heat treated in a tube furnace with wet 100 ppm O_2 gas (bubbler water dew point ~25ºC) through a high temperature conversion step ($T_{conversion}$ = 740ºC-780ºC) under flowing wet 100 ppm O_2/N_2 gas. The film was then cooled under dry 100 ppm O_2/N_2 gas, followed by dry O_2 at 525ºC through cooling to room temperature.

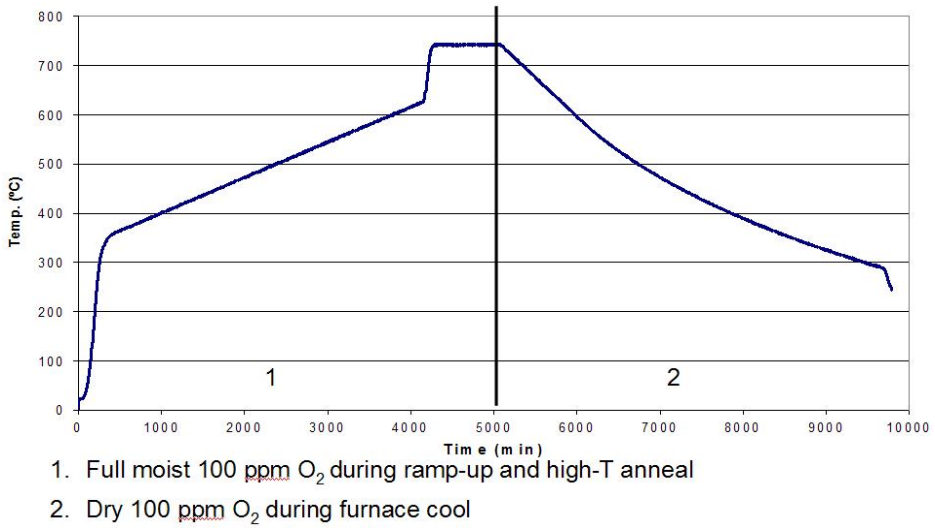

Figure 8. Heat treatment profile for alkoxide-suspension process

2.4.2 Results and Discussion

2.4.2.1 Precursor Results and Discussion

Separate experiments were done to determine whether ultrasonicating, milling, or both would make the most impact in breaking up CuO aggregates, reducing agglomerate sizes, and separating the CuO particles.

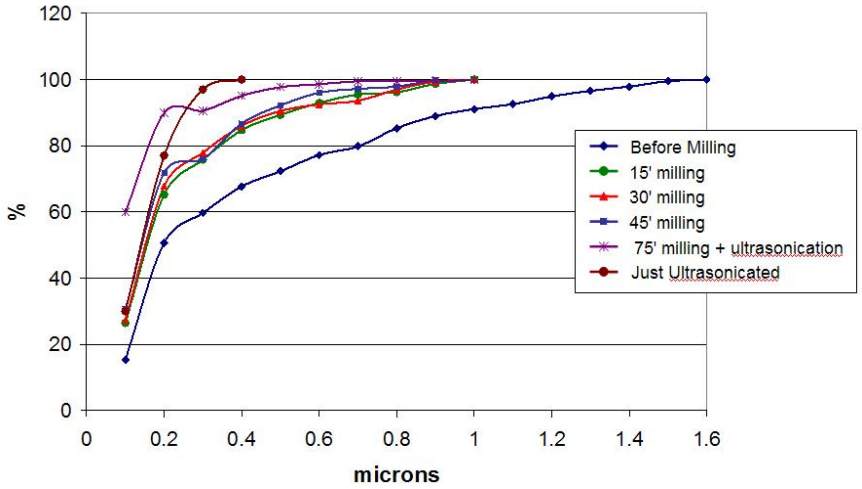

Figure 9. Particle size distributions of CuO nanopowders before and after vibratory milling

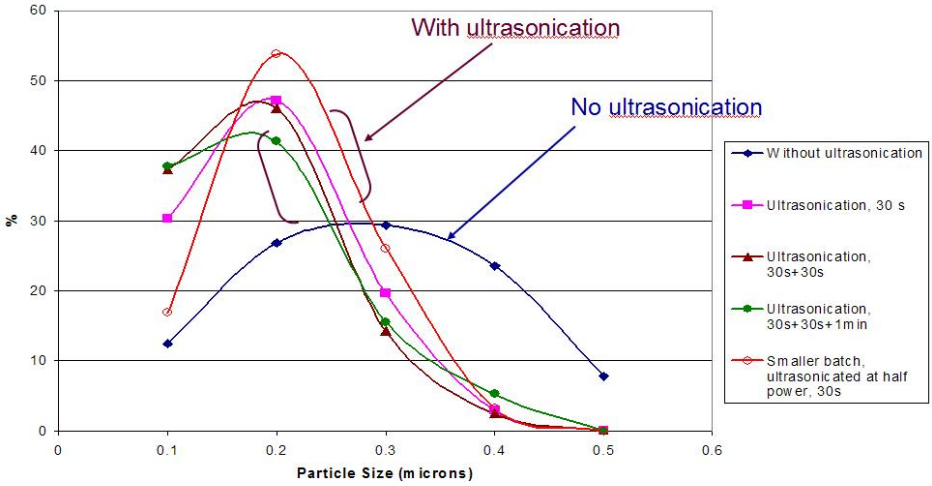

Figure 10. Particle size distributions of CuO nanopowders before and after ultrasonication

It was found that any amount of milling reduced the particle size distribution and broke up aggregates larger than 1 μm. However, the milling time did not make much of a difference. Similarly, any amount of ultrasonication was shown to decrease the particle size distribution, but there was not much of a difference made by ultrasonicating for longer times. A combination of ultrasonication and milling was shown to decrease the particle size distribution approximately the same amount as milling. There was no apparent advantage in combining the two processes. Milling, however, involved the use of media of a different material, and contamination was more likely. Thus, ultrasonication was chosen as the method for breaking up the CuO aggregates and agglomerates.

Different non-ionic dispersant materials were tested for suspension of the CuO in 2-methoxyethanol. The dispersants tried included sorbitan monolaurate (Span 20), sorbitan laurate (Arlacel 20), Surfynol DF210 defoamer, sorbitan oleate (Span 80), and polyethyleneimine (PEI). These suspensions were stirred and left for at least one week to observe the sedimentation behavior of the particles and agglomerates.

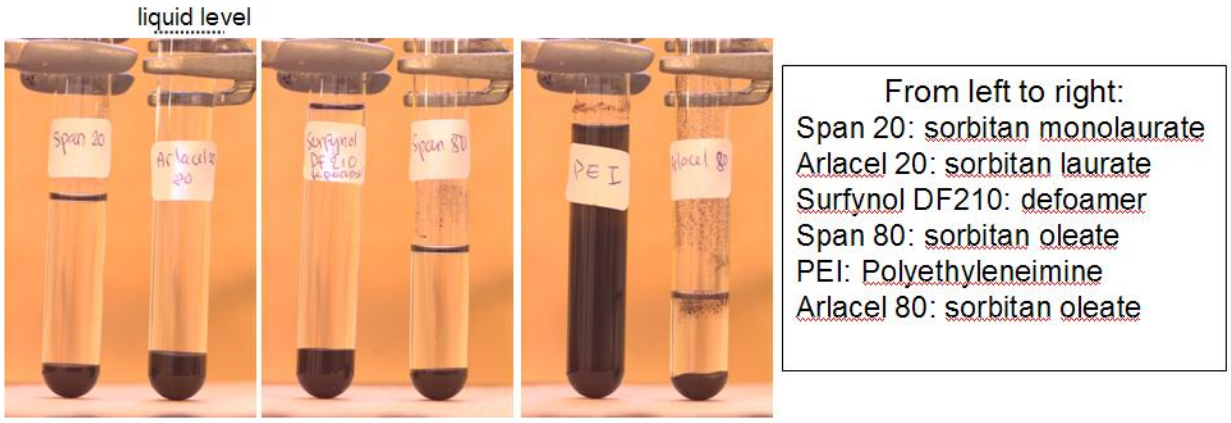

Figure 11. Sedimentation of CuO nanopowder with different dispersants

PEI was found to be the most effective dispersant for CuO nanopowders in 2-methoxyethanol. The amine groups in PEI, and the evidence that it worked well in dispersing CuO, suggested acidic surfaces of the CuO particles.

Optical micrographs showed the differences between films spin-coated from solutions containing CuO that (1) did not have any dispersant and was not ultrasonicated, (2) had dispersant but was not ultrasonicated, and (3) had both dispersant and was ultrasonicated.

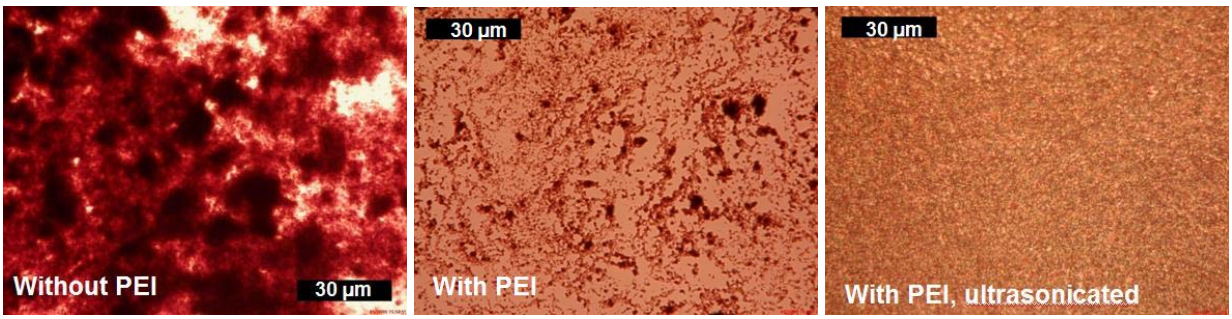

Figure 12. Films spin-coated from different CuO suspensions

These micrographs showed the advantage of having both a mechanical way to separate the CuO powder agglomerates and to keep them separated by the addition of a dispersant. PEI dispersant

did keep agglomerates and particles separated, but there was still a high degree of non-uniformity across the surface of the spin-coated film. Ultrasonicating would allow for larger agglomerates and aggregates to break up, and then the PEI would keep them apart and keep the suspension stable. A combination of both was used for the CuO particles in the final precursor solution.

2.4.2.2 Processed Film Results

The alkoxide-based precursor was more successful in building up film thickness than the TMA precursor solution. Multiple coatings resulted in film thicknesses up to 1 μm (for a six-layer film). It seemed that the first spin-coated layer adhered better to the substrate, because no dewetting was observed. Additional layers also did not seem to dissolve the preceding layers, because the thickness did increase significantly with multiple spin-coating steps. However, thicker films were observed to experience cracking, which posed a serious problem for the current-carrying performance of the films.

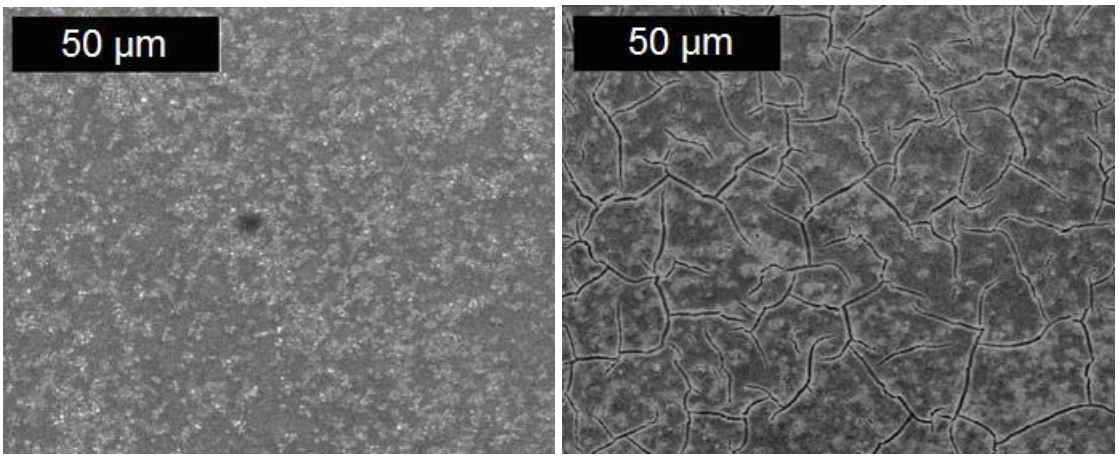

Figure 13. SEM micrographs showing a single-layer (left) and four-layer (right) film

The alkoxide-suspension precursor produced films containing c-axis YBCO, but other compounds, including Cu_2O and an off-stoichiometry Y-Ba-Cu compound, likely $YBa_3Cu_2O_{6.5+x}$

were detected by XRD. These secondary phase peaks were not detected in XRD of films made from precursors that were processed with ultrasonication and dispersion steps.

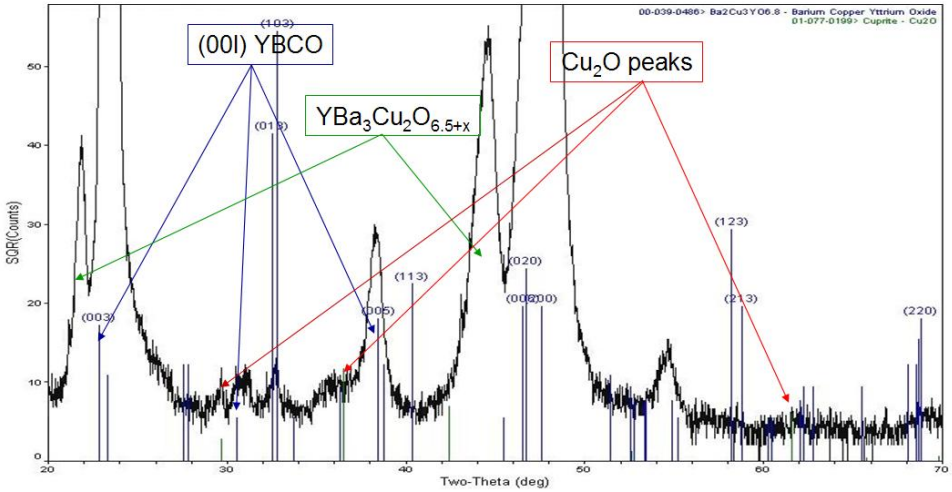

Figure 14. XRD pattern of YBCO film from alkoxide-suspension precursor (not ultrasonicated)

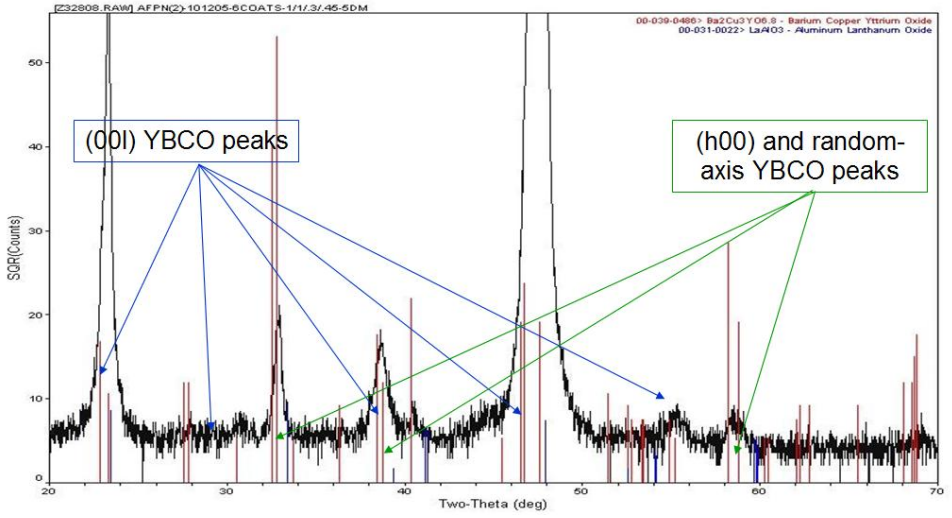

Figure 15. XRD pattern of YBCO film from alkoxide-suspension precursor (ultrasonicated and dispersed)

Despite the observation of clear c-axis YBCO peaks, these films did not carry current because there was no continuous path for the current. The optical micrograph below still showed surface non-uniformities, and an overall discontinuity in the film.

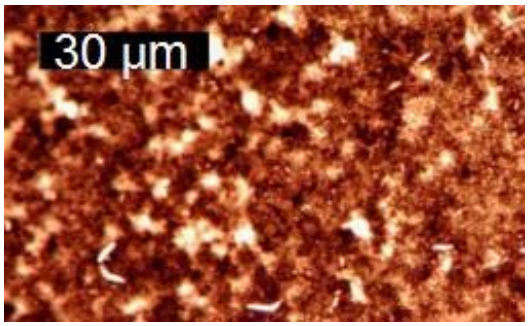

Figure 16. Optical micrograph of YBCO film made from alkoxide-suspension precursor

The alkoxide-based process was promising in that it can be used to produce thick films and was observed to produce c-axis textured YBCO. However, the size of the CuO particles in the precursor solution remained a large problem. Without significantly increasing the extent of mechanical separation and dispersion of the agglomerates, the films produced would remain non-uniform and there would be patches where there is no film at all, as observed above. This further complicated the process. Although it was possible to decant only the smallest and most dispersed CuO particles after ultrasonicating and dispersing, the overall stoichiometry control would become much more difficult. This process initially seemed to offer more advantages than the TMA process, but it was not the most promising solution, because it did not produce current-carrying YBCO films.

2.5 Polymer-Nitrate Precursor Solution

The third solution deposition system tested was an aqueous polymer-nitrate system. Work done previously had successfully deposited CeO_2 films on single-crystal YSZ substrates using a

polymer-nitrate solution [35]. Using this work as a starting point, aqueous solutions of Y, Ba, and Cu nitrates and various polymers were made and tested for their viability in making sufficiently thick, current-carrying YBCO films.

2.5.1 Experimental Procedure

2.5.1.1 Precursor Solution Preparation

The polymer-nitrate precursor solutions used yttrium nitrate hexahydrate ($Y(NO_3)_3 \cdot 6H_2O$, MW 382.94 g), copper nitrate trihydrate ($Cu(NO_3)_2 \cdot 3H_2O$, MW 241.57 g), and barium nitrate ($Ba(NO_3)_2$, MW 261.35 g). These nitrate powders were dissolved in deionized water, making a light blue solution with 0.3-0.8 M total cation concentration. A polymer rheology modifier was used to modify the wetting behavior and thickness of the deposited film. Polymers such as polyvinyl alcohol (PVA), polymethylmethacrylate (PMMA), polyacrylic acid (PAA), and methyl cellulose were initially tried as candidates for the rheology modifier. It was found that out of these polymers, PVA and methyl cellulose both could be used to produce continuous films of sufficient thickness that wet the substrates.

PVA-nitrate solutions were prepared by adding PVA (MW 15000) to an aqueous solution of the nitrates under heat and stirring. Approximately 5-10 wt% PVA with respect to the total weight of the nitrate-water solution (~63-125 wt% with respect to the total nitrates, depending on the solution concentration) was added before the solution reached 40^{o}C, resulting in a cloudy light blue solution. The cloudy solution became clear at around 80^{o}C, after which the solution was taken off of the hot plate to cool. The finished precursor solution was a viscous, clear light blue solution. Methyl cellulose-nitrate solutions were prepared by pouring a heated (~80º) aqueous nitrate solution onto 2-10 wt% methyl cellulose with respect to water while mixing. The

whole solution was then mixed at room temperature and allowed to cool. The nominal stoichiometric ratios of the solutions were Y: Ba: Cu = 1: 1.8-2: 3.

2.5.1.2 Deposition and Heat Treatment

The polymer-nitrate solutions (polymer: PVA or methyl cellulose) were spin-coated onto LAO substrates at a speed of 4000 rpm for 120 s. The spin-coated films were then heat-treated up to T_{anneal} = 760ºC under flowing 100 ppm O_2/N_2 atmosphere, followed by flowing dry O_2 gas during furnace cooling to room temperature.

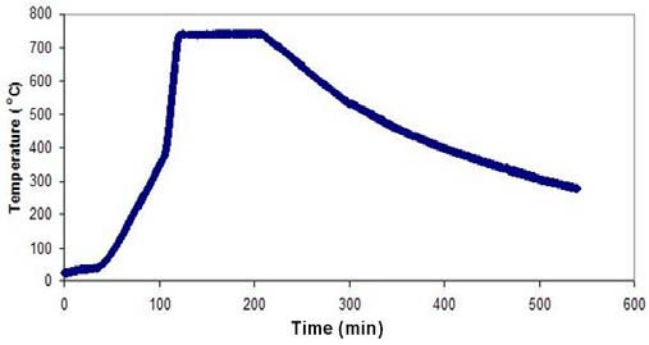

Figure 17. Polymer-nitrate heat treatment profile

2.5.2 Results and Discussion

A summary of the thickness, J_c, and observations of the various polymer-nitrate solutions is presented in the table below.

Table 2. Summary of results for polymers as rheology modifiers in nitrate solution

Polymer	Wt % (wrt H_2O)	Thickness	MA/cm^2 J_c?	Remarks
PVA	5-10%	<100 – 250 nm	Yes	Limitations in final film thickness
MC	2-10%	<100 to 350 nm	Yes	Purity problems with available grades.
PAA	1-2%	Not continuous	No current	Film dewetting, patchy film
PMMA	3-10%	Not applicable	N/A	Unspinnable precursor solution

Both the PVA and methyl cellulose dissolved nicely to produce viscous aqueous solutions, while neither PMMA nor PAA were suitable for the aqueous nitrate solution. PMMA did not significantly increase the viscosity of the solution to a point where it could be spin-coated into a film. A viscous PAA-nitrate solution did not sufficiently wet the substrate to produce a continuous green film. PVA and methyl cellulose were both used in precursor solutions that produced c-axis textured, current-carrying YBCO films with thicknesses over 100 nm. Similar solutions were made from the nitrates of holmium, barium, and copper, and also produced c-axis, high performance (J_c > 1 MA/cm$_2$) HoBCO films.

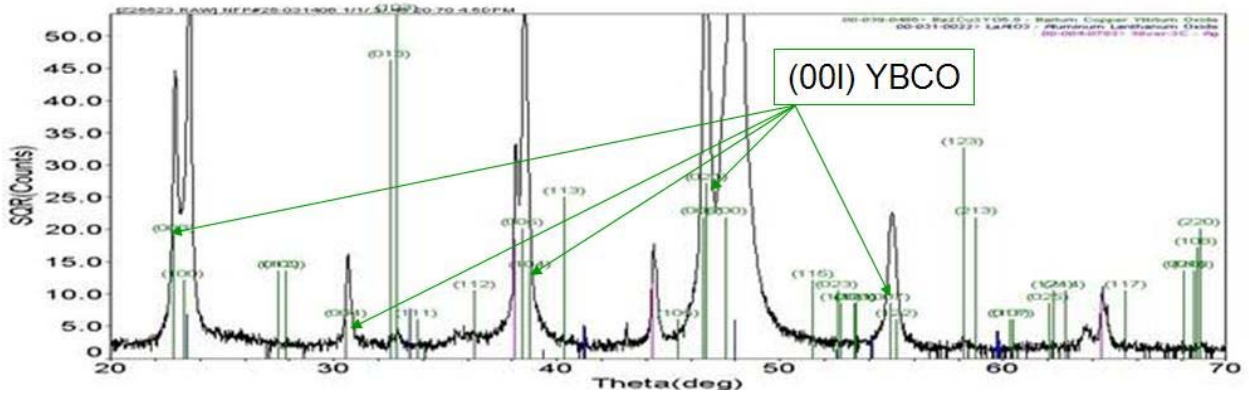

Figure 18. XRD pattern of YBCO film made from PVA-nitrate solution

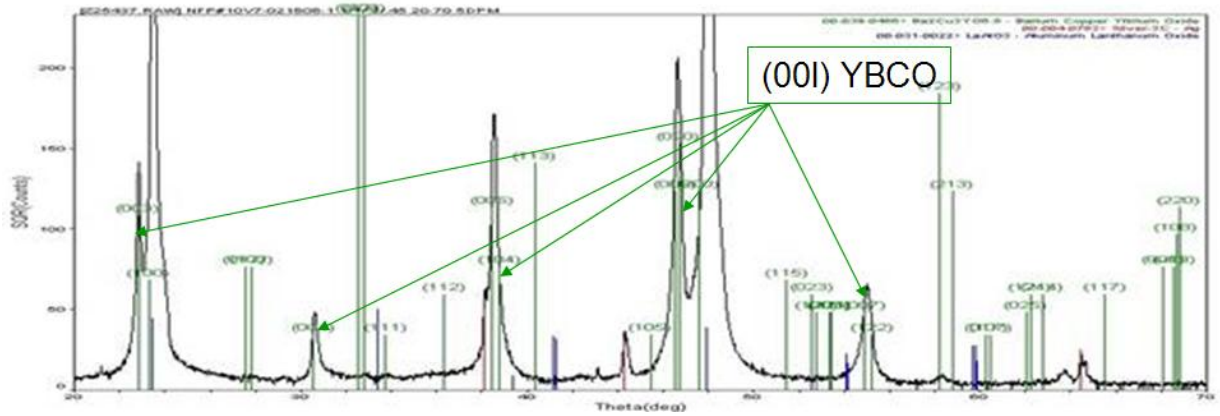

Figure 19. XRD pattern of YBCO film made from methyl cellulose-nitrate solution

The polymer nitrate precursor solution clearly possessed advantages compared to the two other processes. The solution preparation was straightforward and did not require an intermediate reaction step such as that found in the TMA process. The solution was uniform and produced sufficiently thick, current carrying YBCO films. Based on these initial results, the polymer nitrate precursor solution was selected to be the solution that would be developed throughout the rest of this thesis work. The development of this precursor solution system will be discussed in the Chapter 3, and the evolution of the microstructure of resulting films and their relationship to film performance will be discussed in Chapter 4.

CHAPTER 3: POLYMER-NITRATE PRECURSOR SOLUTION DEVELOPMENT

3.1 Limitations of the Polymer-Nitrate Precursor Solution

The polymer-nitrate solution was the only one of the three different solution systems tested in the previous section that produced current-carrying YBCO films. However, the solution was far from perfect. Initial film thicknesses seemed to stop at ~250-350 nm, and the reproducibility of films with $J_c > 1$ MA/cm^2 was still quite low. The solubilities of yttrium nitrate and copper nitrate in water are both more than 130 g in every 100 g of water, while the solubility of barium nitrate is only ~10 g for every 100 g of water [47]. Supersaturation of barium nitrate in solution resulted in precipitation of crystalline barium nitrate within the deposited films as they dried during and after spin-coating. This crystallization of barium nitrate became more apparent over time, as was seen in the formation and growth of dendritic structures in the films.

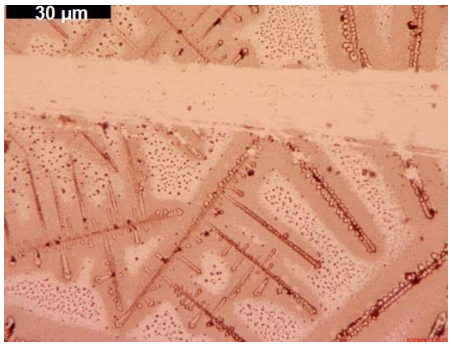

Figure 20. YBCO film with $Ba(NO_3)_2$ crystallization

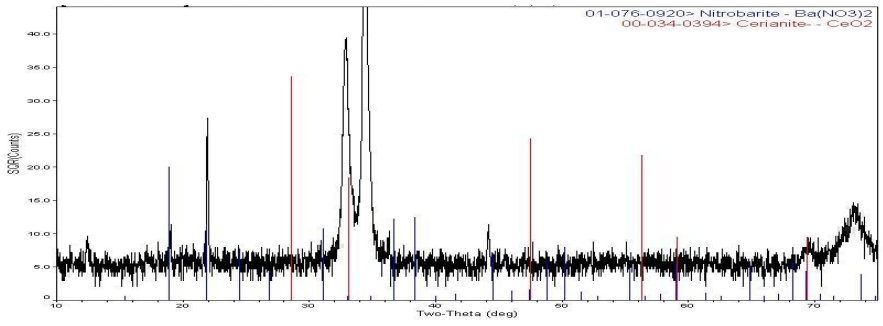

Figure 21. XRD pattern confirming presence of $Ba(NO_3)_2$ crystals

The second specific aim of this thesis work was to address these limitations in the precursor solution in order to improve the YBCO film performance and increase reproducibility of the high performance films. Modifications to the precursor solution were made to address the different precursor solution limitations, and a latest version of the polymer-nitrate precursor solution was obtained. Recommendations for additional improvements that can be further made to this precursor solution are discussed at the end of the chapter.

3.2 Effect of PVA on Film Thickness

3.2.1 Experimental Procedure

Changes in the viscosity of the precursor solution were hypothesized to be related to the amount of polymer, and in turn the viscosity of the solution would affect the thickness of the deposited precursor film. The initial work covered in Chapter 2 showed PVA to be a promising rheology modifier. Viscosity measurements of PVA-nitrate solutions with different PVA amounts were conducted. Measurements of green and fired film thicknesses were related to the viscosities of the solutions used to obtain those films.

3.2.2 Results and Discussion

The viscosity of solutions containing different amounts of PVA rheology modifier increased with higher PVA content. However, higher viscosity did not necessarily mean higher final film thicknesses; the slight increase in thickness with viscosity leveled off around 200 nm.

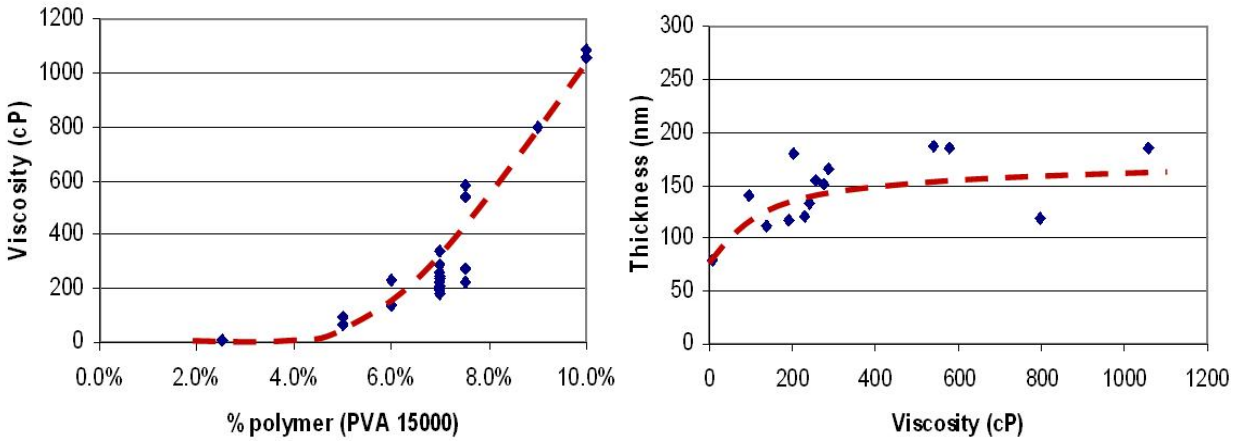

Figure 22. Higher PVA content increases viscosity, but doesn't significantly increase final thickness

These results suggested that further increasing the film thickness would require more than just increasing the viscosity of the solution. The total cation concentration of the PVA-nitrate precursor solution would have to be increased from its ~0.3 M value to increase the amount of cations deposited onto the substrate. The low solubility of $Ba(NO_3)_2$ posed a challenge in achieving this goal. Approaches to dealing with $Ba(NO_3)_2$ crystallization as a result of supersaturation of $Ba(NO_3)_2$ in solution are discussed in the next section.

3.3 Reducing or Eliminating $Ba(NO_3)_2$ Crystallization

3.3.1 Experimental Procedure

Several experiments were conducted with the goal of reducing or eliminating $Ba(NO_3)_2$ crystallization from the precursor film. The crystallization had to be prevented during and after spin-coating, as well as up to a temperature (< 300ºC) at which the film became stable under ambient conditions and no further crystallization would occur. The first experiment involved addition to the viscosity of the precursor solution and mechanically preventing segregation of

$Ba(NO_3)_2$ crystals out of the spin-coated film. This was done by adding the amount of PVA in PVA-nitrate solutions, and observing the change(s) in the appearances of the spin-coated films.

The second experiment involved addition of polyethylene glycol (PEG) as a chelating agent. Different amounts of different molecular weight PEG were added to solution aliquots, and the resulting spin-coated film observed at a 500x magnification using an optical microscope in reflection mode. Work done on other systems showed that it was possible to use compounds such as polyethylene glycol (PEG) to chelate with metal cations. Work by Rogers et al, for instance, used PEG as an extracting agent for Sr^{2+} cations from aqueous solutions of $Sr(NO_3)_2$ and $SrCl_2$ [48].

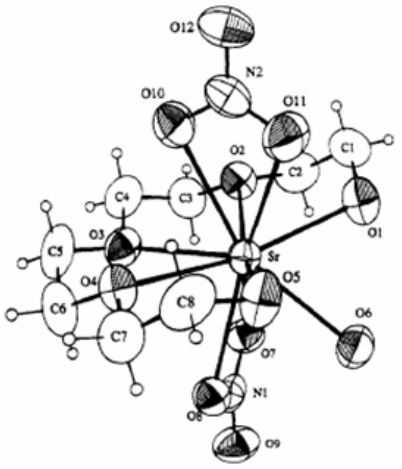

Figure 23. Schematic of PEG chelation of Sr^{2+} cation [48]

The third experiment was done with the goal of preventing $Ba(NO_3)_2$ crystallization at elevated temperature. A later version of the precursor solution used hydroxypropyl methyl cellulose (HPMC) as its rheology modifier (see Section 3.4). PEG as a chelating agent prevented $Ba(NO_3)_2$ crystallization during and after spin-coating, but crystallization was observed in post-heat treated films. Considering that PEG chelated well with Ba^{2+} cations in solution, a second

chelating agent, and not a replacement chelating agent, was sought to prevent crystallization during heat-treatment.

3.3.2 Results and Discussion

3.3.2.1 Rheology Modifier Addition

Increasing the PVA content of the precursor solution was found to reduce the extent of $Ba(NO_3)_2$ crystallization. The following optical micrographs showed a stark difference between films made from solutions containing 6 wt% and 10 wt% PVA. The viscosity of the latter solution was approximately five times that of the former. Clearly, while viscosity increase did not increase final film thickness, it did affect this characteristic of the films.

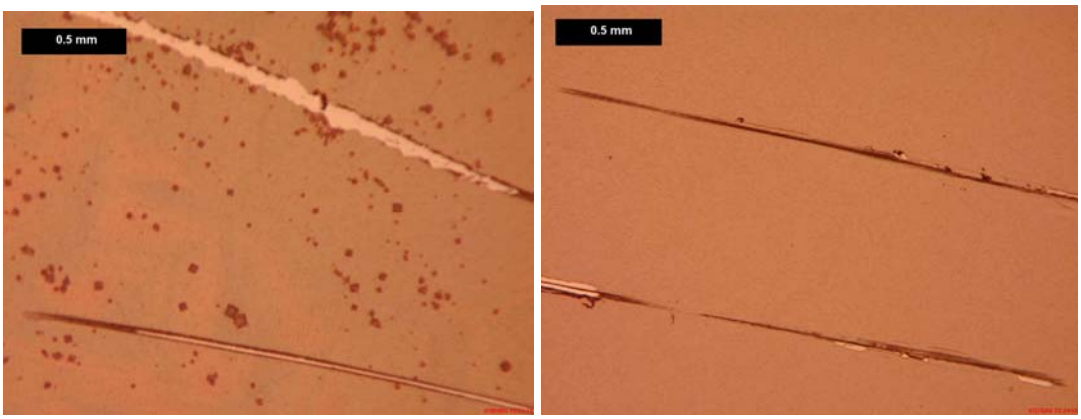

Figure 24. PVA-nitrate films spin-coated under similar conditions (dew points 12.5ºC and 12.7ºC, respectively), showing the difference between having 6 wt% PVA (left) and 10 wt% PVA (right)

It had been observed that with higher ambient humidity, films tended to experience more crystallization. This may be because the slow drying of the film allowed the $Ba(NO_3)_2$ crystals to grow and form the dendritic structure observed even at lower magnifications. However, addition of PVA resulted in a lesser extent of the growth of the dendrites, even under those higher humidity values. The resulting increase in viscosity of the solution, as discussed above,

mechanically prevented the crystallites from growing. However, this addition was not completely effective in preventing the $Ba(NO_3)_2$ crystals from nucleating.

Figure 25. A PVA-nitrate film made from a 10 wt% PVA solution, showing small $Ba(NO_3)_2$ nuclei and one that had formed into a dendritic feature

Finally, there was only so much PVA that could be added to the solution before it became too viscous to pipette onto the substrate for spin-coating. Another method for preventing $Ba(NO_3)_2$ crystals from forming and growing would have to be used.

3.3.2.2 Addition of PEG as a Chelating Agent

The optical micrographs presented below showed the differences between films made from PVA-nitrate solutions containing 5 wt% and 7 wt% PEG 400, and 7 wt % and 10 wt% PEG 1500, respectively.

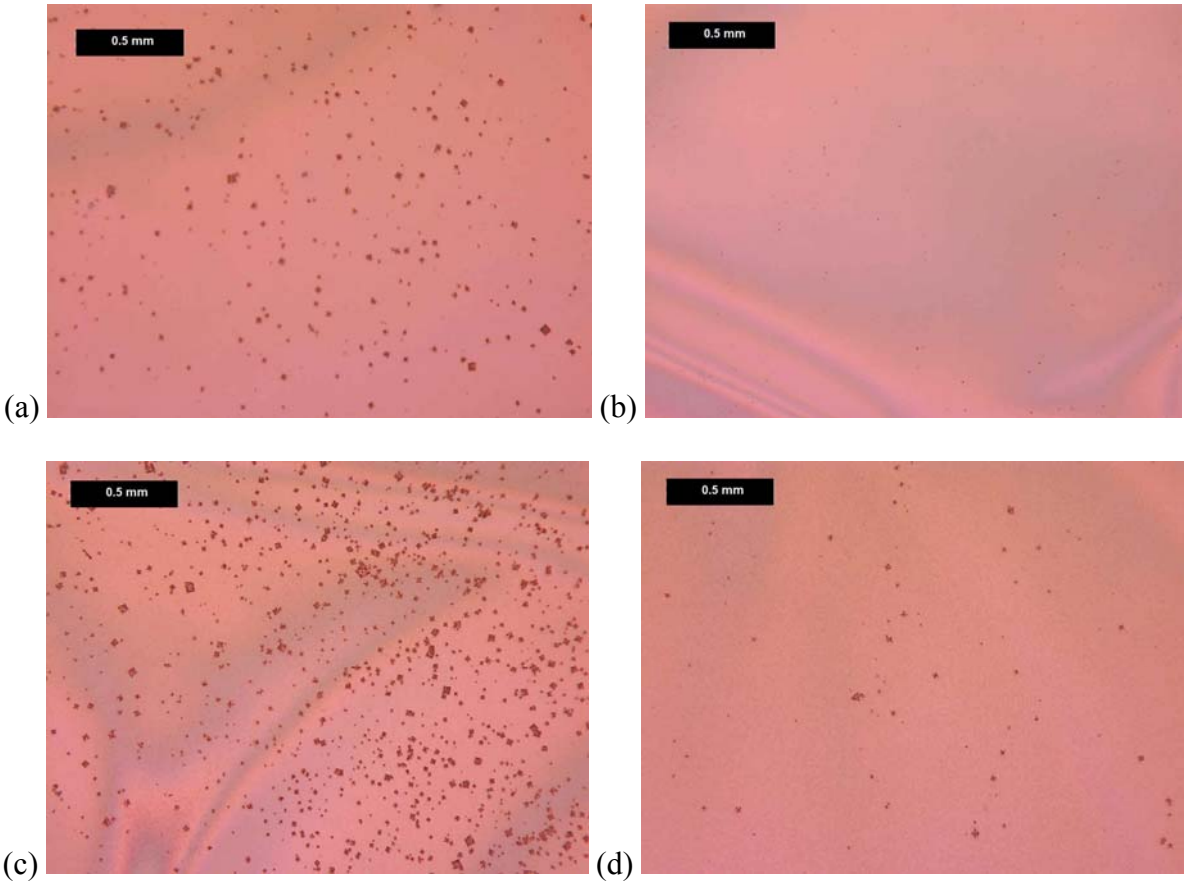

Figure 26. Optical micrographs of films made from PVA-nitrate solutions containing (a) 5 wt% PEG 400, (b) 7 wt% PEG 400, (c) 7 wt% PEG 1500, and (d) 10 wt% PEG 1500

The addition of PEG as a chelating agent significantly suppressed $Ba(NO_3)_2$ crystallization in both cases. The lower molecular weight PEG was more effective in suppressing crystallization than the higher molecular weight PEG. Furthermore, while adequate amounts of PEG were required to chelate with the Ba^{2+} cations, too much of it resulted in more crystallization. An explanation may be found in the comparison of the viscosities of PVA-nitrate solutions with different amounts of PEG400.

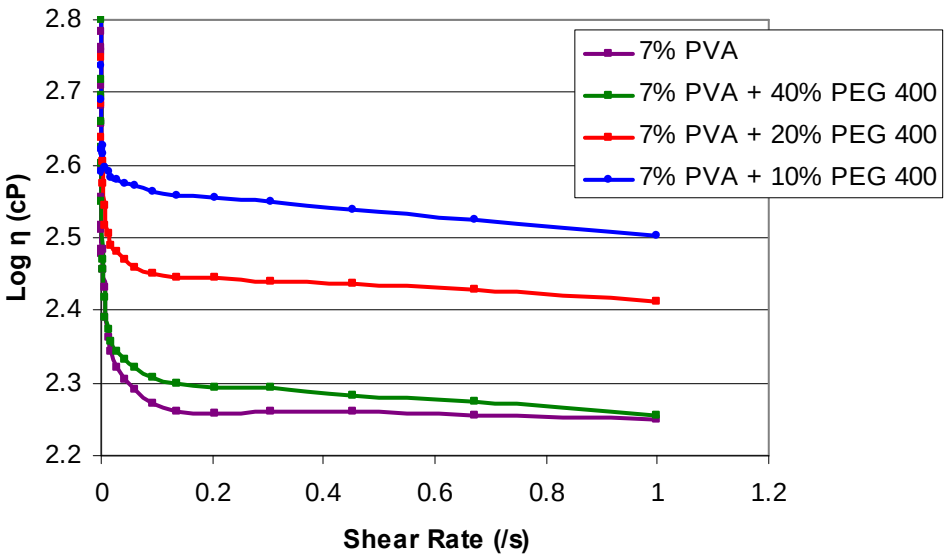

Figure 27. Viscosities of PVA-nitrate solutions containing 0%, 10%, 20%, and 40% PEG 400

PEG not only served an important role as a chelating agent for the Ba^{2+} cations, it also acted as a plasticizer [4951,66], thereby decreasing the overall viscosity of the solution and allowing for more mobility within the film as it was deposited. Any $Ba(NO_3)_2$ nuclei that formed would be more likely to grow, given high percentages of PEG (≥40%). There was a trade-off between having enough chelating agents to prevent $Ba(NO_3)_2$ crystallization, and maintaining the viscosity necessary to obtain the desired film thickness and to help further mechanically prevent crystallization. The rest of the discussion on solutions from this point on will automatically assume inclusion of low-molecular weight PEG as a chelating agent in any precursor solution, regardless of the choice for rheology modifier.

3.3.2.3 Preventing Crystallization during Heat-Treatment

A second chelating agent was needed to prevent crystallization of $Ba(NO_3)_2$ after low-temperature heat treatment. Spin-coated HPMC-nitrate films were heat treated and their optical

micrographs observed. Green spin-coated films from the HPMC-nitrate precursor solution were smooth with no crystallization features. However, when these films were heat treated, significant crystallization features were observed. These low-magnification micrographs are presented in the following figures.

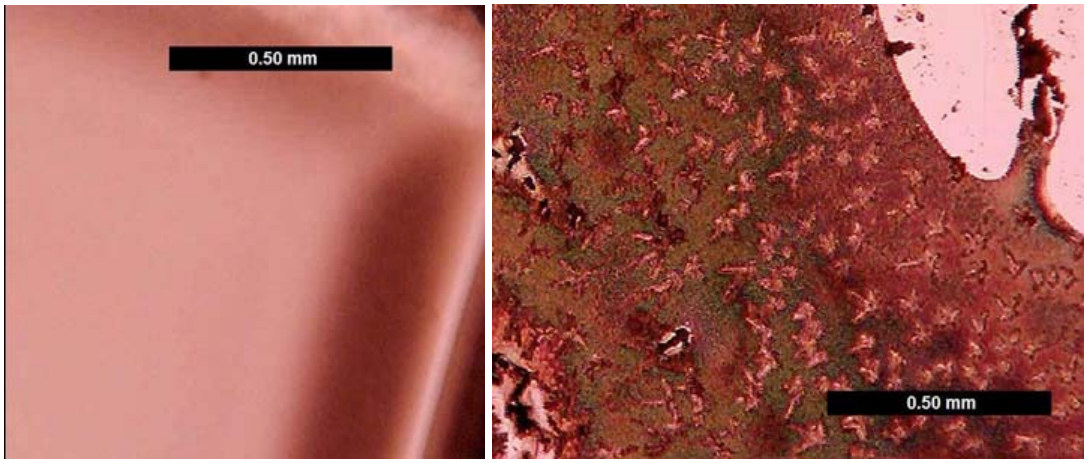

Figure 28. HPMC-nitrate films (left) after spin-coating and (right) after heat treatment

Work done by Yang et al explored the role of sucrose-metal ion interactions in ion binding and transport applications [52]. This was also applicable to the polymer-nitrate system; sucrose was tried as the second chelating agent in the precursor solution. PEG was a more effective chelating agent at room temperature than sucrose. However, the cross-linking reaction that took place upon caramelization of the sucrose [54] prevented crystallization from occurring at elevated temperatures (between 100ºC and 200ºC). The optical micrograph taken after heat treatment showed a uniform, crystallization-free film. The presence of both PEG and sucrose in the HPMC-nitrate precursor solution produced a film that was crystallization-free both after spin-coating and after heat treatment. PEG and sucrose were from this point on used as chelating agents for the polymer-nitrate precursor solution.

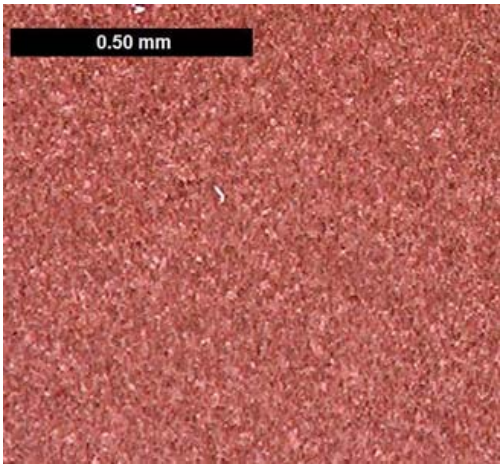

Figure 29. YBCO film made from HPMC-nitrate solution containing PEG and sucrose

3.4 Film Delamination

Most of the experiments for the course of this thesis work were done on single-crystal LAO substrates. However, the coated conductor architecture as previously described involves a buffered metal substrate layer. The precursor solution developed here would have to be able to be applied to buffered metal substrates.

3.4.1 Experimental Procedure

The goal of this particular section was to tailor the precursor such that a continuous YBCO film could be obtained on a buffered Ni/W alloy substrate. The film would have to wet the substrate, not delaminate, and possess adequate thickness. A PVA-nitrate precursor solution as developed in previous sections was initially used. Delamination and de-wetting of the resulting YBCO film were observed. Based on these observations, a search was made for a different rheology modifier that could be used as part of a precursor solution for films that would not delaminate from buffered metal substrates.

3.4.2 Results and Discussion

Films made from PVA-nitrate precursor solutions experienced significant delamination, as shown in the photograph below. The film wets the substrates for the most part. However, the middle section of the film, marked by the red arrow, had peeled off, leaving an exposed section of the substrate.

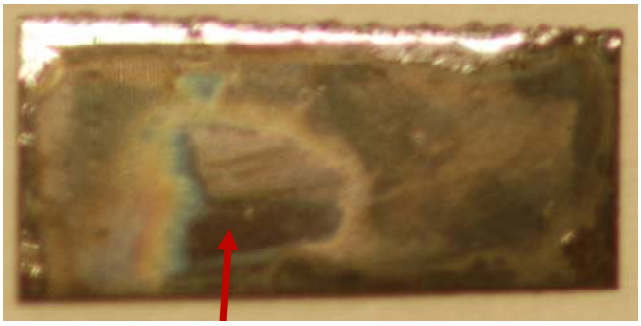

Figure 30. PVA-nitrate based YBCO film on buffered metal substrate, showing delamination

The precursor solution used to make this ~200 nm film had 7 wt% PVA with respect to the amount of water. Any further increase in rheology modifier would not only result in worse delamination but would also not significantly raise the film thickness. A search was made for a different rheology modifier that could produce the same or greater green thicknesses with lower weight percentages.

Initial polymer-nitrate experiments described in Chapter 2 showed that more than one polymer was feasible for producing current-carrying YBCO films. An alternative to PVA was methyl cellulose, which also produced MA/cm^2 YBCO. Cellulose ethers such as methyl cellulose, hydroxypropyl methyl cellulose (HPMC), and hydroxyethyl cellulose (HEC) were useful in

several ways. They served as stabilizers and thickeners, and lent a thixotropic behavior to the solution [53]. The shear-thinning aspects of the rheological behavior of the solutions that contain these polymers were useful during deposition, and their thixotropic recovery upon standing useful to maintain the deposited precursor film's thickness.

These polymers were found to achieve the same or even greater film thicknesses with only 1-3 wt% with respect to water. Thicker films, up to 600 nm per layer, were made using HPMC-nitrate solutions. A ~400 nm film wet the substrate very well, and did not exhibit the same delamination behavior as the PVA-nitrate films did on the buffered Ni-W substrate.

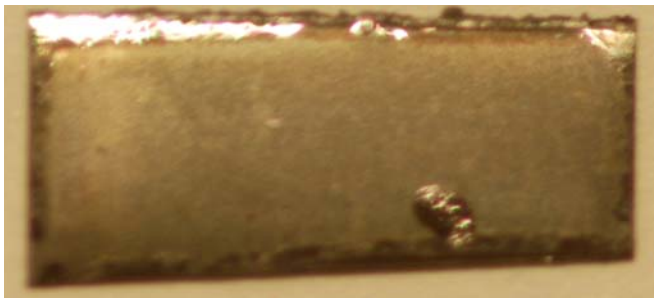

Figure 31. HPMC-nitrate based YBCO film on buffered metal substrate, showing no delamination

The presence of PEG as a plasticizer in the low weight% HPMC solution also increased the toughness and tear resistance of the film [50]. HPMC-nitrate precursor solutions were preferable to PVA-nitrate solutions, both because they formed films that adhered well to metal substrates and because there were more possibilities for increasing the final film thickness with less % rheology modifier.

3.5 Film Cracking and Organic Content

The different modifications and additions to the polymer-nitrate precursor solution resulted in quite a bit of total organics, significantly exceeding twice the amount of nitrates: the

rheology modifier (~1-3 wt%), PEG (~30 wt%), and sucrose (~30 wt%). These percentages are weight percentages with respect to the water. HPMC-nitrate films could produce ~600 nm individual film layers, but at higher thicknesses these films experienced significant cracking.

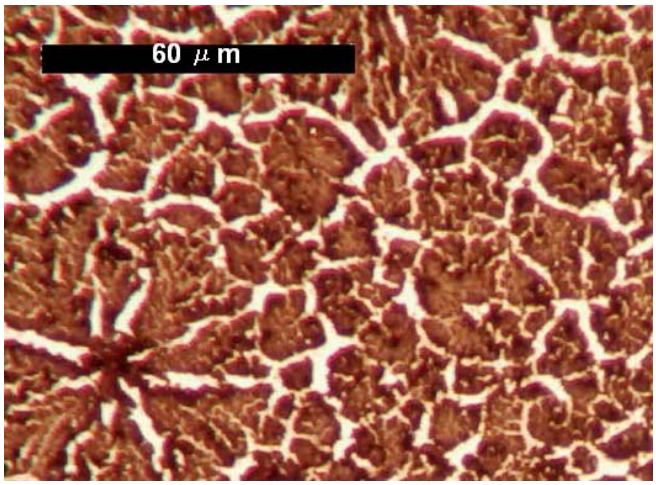

Figure 32. Optical micrograph of HPMC-nitrate film with severe cracking (most samples with cracking problems had less extensive cracks)

The large change in volume as the organics were decomposed and removed from the film produced large strains in the film that led to cracking. Solving this problem required a reduction of the total amount of organics without compromising the chelation of cations in the solution and precursor film.

3.5.1 Experimental Procedure

A method for reducing total organic content while maintaining the chelation of cations was explored. The solubility of $Ba(NO_3)_2$ in water at 20ºC is only 9.02 g/100 g H_2O, but more than doubles to 27.2 g/100 g H_2O at 80ºC [47]. A modified solution was made that contained only a total of ~12 wt% organics as opposed to ~36 wt%. This solution was stored at room

temperature to prevent significant decrease in viscosity due to the degradation of the rheology modifier. $Ba(NO_3)_2$ precipitated out of solutions with low chelator content at room temperature. Prior to deposition, the precursor was heated to ~80ºC until the $Ba(NO_3)_2$ precipitates were re-dissolved into solution. This heated precursor solution was then deposited onto the single-crystal substrates with the procedure described previously.

Additional measures were taken to assist in preventing $Ba(NO_3)_2$ crystallization from the spin-coated films. Spin-coating was done in a nitrogen glove box, and films were further dried with a small vacuum set-up immediately after deposition. These films were heat-treated to 275ºC in order to produce films that would be stable in ambient atmospheres before further processing, including a final heat treatment to form YBCO.

3.5.2 Results and Discussion

The modified precursor solution containing about half the required chelating agents had to be heated prior to spin-coating deposition. However, the HPMC rheology modifier was insoluble at elevated temperatures. HEC is soluble at both low and elevated solution temperatures, and is also an effective rheology modifier. The viscosity of a 3 wt% HEC solution in water was found to be higher than the viscosities of the 7 wt% PVA solutions at higher shear rates. This led to small additions of HEC resulting in higher deposited film thicknesses. HEC was therefore chosen as a rheology modifier to replace HPMC.

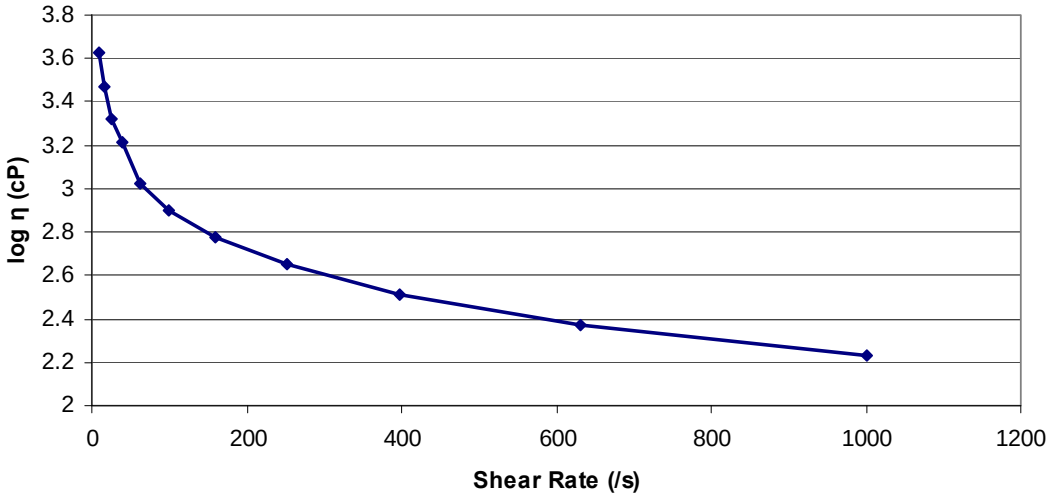

Figure 33. Viscosity of 3 wt% HEC solution in water

The films produced from heated HEC solutions with reduced total chelator content were comparable to those produced from solutions with ~60 weight% chelating agents with respect to the water. The thicknesses of films with 1.2 wt% HEC and cation concentration ~0.6 M were 338 nm for films made from the high chelator content solution, and 416 nm for those from low chelator content solution. The high cation concentration could be maintained even with lower chelator content with this elevated-temperature solution arrangement. The J_c values of films made from the high chelator content HPMC-nitrate precursor solution and those made from the low chelator content HEC-nitrate precursor were comparable. Films made from both solutions reproducibly exceeded 1 MA/cm^2, with the latter films reaching higher single-layer thicknesses.

Spin-coating in a nitrogen glove box, followed by further fast drying of the film under vacuum, further improved the uniformity of the green films. This method allows for even further reduction in the amount of chelating agents in the precursor solution. A precursor solution with a total of ~20 wt% chelating agents and 1.8 wt% HEC was spin-coated to produce a green film that did not show evidence of $Ba(NO_3)_2$ crystallization. This film, as well as other HEC-nitrate films

spin-coated in the nitrogen glove box, was heat treated to 275ºC to obtain an ambient atmosphere-stable film that could be further processed to produce the final YBCO film.

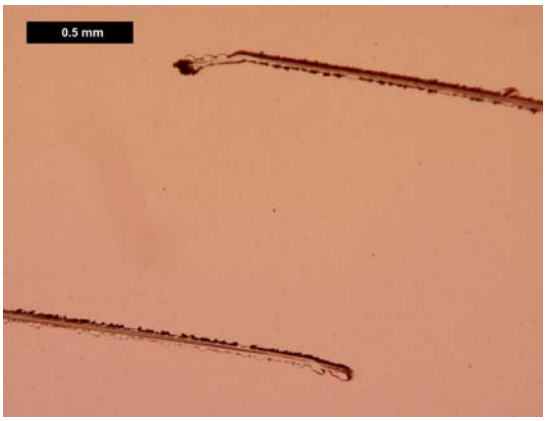

Figure 34. Optical micrograph of a precursor film with no $Ba(NO_3)_2$ crystallization

3.6 Final Solution Preparation

The polymer-nitrate precursor solution had to be modified in response to the different problems observed with the spin-coated precursor and final films. The final precursor solution had HEC as its rheology modifier, and low molecular weight PEG (PEG 200) and sucrose as chelating agents for the cations. A 3 wt% aqueous HEC solution was prepared in ~50-60 mL batches. Mixing was done overnight to obtain a uniformly dissolved, viscous HEC solution. 15 mL batches of the solution were centrifuged at ~8000 rpm for 15-20 minutes to separate out insoluble fibers found in the as-received HEC. Approximately 8 g of the clear, fully soluble part of the solution was then mixed with 0.653 g of $Ba(NO_3)_2$ (Alfa Aesar), ~0.8 g PEG 200, and distilled water to make a total of ~11 g of solution. Mixing was done until most of the $Ba(NO_3)_2$ crystals appear to be dissolved. The solution was then heated to ~40-50ºC while 0.478 g of $Y(NO_3)_3 \cdot 6H_2O$ and 0.906 g $Cu(NO_3)_2 \cdot 3H_2O$ were stirred into the solution. Finally, ~0.8 g of sucrose was added to the solution, and it was stirred and heated to ~80ºC for 45-60 minutes until

a fully uniform, clear light blue solution was obtained. Aliquots (2-3 mL) of the hot solution were taken and placed into smaller vials containing individual spin bars. These individual solution vials were then stirred and heated to ~80ºC for up to one hour prior to spin-coating to re-dissolve the $Ba(NO_3)_2$. The final precursor solution had a Y: Ba: Cu ratio of 1: 2: 3 and a total cation concentration between 0.7 – 0.8 M. The total organic content was about 12 wt% with respect to the entire solution.

3.7 Summary

A final precursor solution was obtained that was used to reproducibly obtain 300 nm or thicker YBCO films with MA/cm^2 critical current densities. Films as thick as 800 nm per layer were also obtained. Heating of the precursor solution prior to spin-coating allowed for reduced amounts of the additives, and improved the properties of the resulting YBCO films.

CHAPTER 4: HEAT TREATMENT AND ANALYSIS

4.1 Introduction

The third specific aim of this thesis will be to develop high performance (> 1 MA/cm^2 critical current density) YBCO films from the non-fluorine precursor solution described in the previous chapter. Emphasis was placed on developing a low temperature (under 500ºC) process to obtain high quality intermediate films that would then be converted to the high performance final YBCO films. The low temperature process is important, because defects in the form of barium nitrate crystallization or cracking would prevent the formation of high performance final films altogether. A number of analytical techniques were used to determine the chemical changes taking place in the film as it was heated up from the precursor state. This knowledge was used to tailor the low temperature heat treatment that would be used on the film prior to its high temperature conversion. YBCO films with I_c values of over 50 A/cm and J_c values exceeding 1 MA/cm^2 were obtained with this process, completing the main goal of this thesis work.

4.2 Film Deposition

4.2.1 Experimental Procedure

The finished precursor solutions were portioned into 3 mL vials. Each vial was heated immediately prior to spin-coating for one hour at ~80ºC on a hot plate with a magnetic stirrer. The heating procedure was done to re-dissolve the barium nitrate crystals that have precipitated out of solution when the solution was stored at room temperature. Solution deposition was done using a photoresist spin-coater. Three to four drops of solution were dripped onto 8 mm x 8 mm single crystal $LaAlO_3$ (LAO) substrates, which were then spun at 4000 rpm for 60 s. All of this

was done inside a dry nitrogen glove box. Optical micrographs were taken with a Nomarski filter to closely observe any defects on the film surfaces.

4.2.2 Results and Discussion

Surface defects in the film were primarily formed during the decomposition temperature range, including bubbles and Bénard cells [51]. Bubbles were formed during the rapid evolution of the gases during heating. Bénard cells resulted from the differences in surface tension in different parts of a film as a result of the reactions taking place as the film was heat treated. The cell formation was especially problematic in thick (>2.5 μm) decomposed films. Thicker films exhibited bubbles in addition to Bénard cells, a result of the different surface tensions of the center and edges of the film and trapped gas from the thicker film edges. Films with decomposed thicknesses between 1.5 and 2.5 μm yielded good quality intermediate films. These produce YBCO films of less than 0.6 μm after conversion.

The supersaturation of barium nitrate in solution gave an additional challenge. Some films were observed to still have some barium nitrate crystallization features on their surface, even though they were spin-coated in a dry nitrogen glove box. The spin-coated film still required time to dry, and during that time there was enough mobility in the film to allow barium nitrate crystallization to take place and dendrites to grow, especially in thicker films (> 2.5 μm).

An additional method to speed up the drying process was required. Placing the film on a hot plate immediately after spin-coating was not an acceptable solution to the problem. The fast evolution of bubbles at an elevated temperature (~80ºC) resulted in a film with bubbles (Figure 35 (a)). Films spin-coated from solutions containing high amounts of sucrose had been shown to produce Bénard cells on the film surface due to the surface tension that resulted from a cross-

linking reaction associated with the thermal decomposition of sucrose. Heating the film on a hot plate immediately after spin-coating exacerbated this problem. The rapid evolution of gas coupled with differences in surface tension across the film resulted in Bénard cells and bubbles (Figure 35 (b)).

A room-temperature fast drying step that involved a vacuum system was then introduced. Each spin-coated film was placed under a glass apparatus connected to a vacuum and dried immediately after deposition. Films dried under vacuum for longer than 3 minutes were also found to have bubbles, so the vacuum drying step was done for only about 1-1.5 minutes. This was found to be adequate to produce green films that were smooth and effectively free of barium nitrate crystals and other surface defects (Figure 35 (c)).

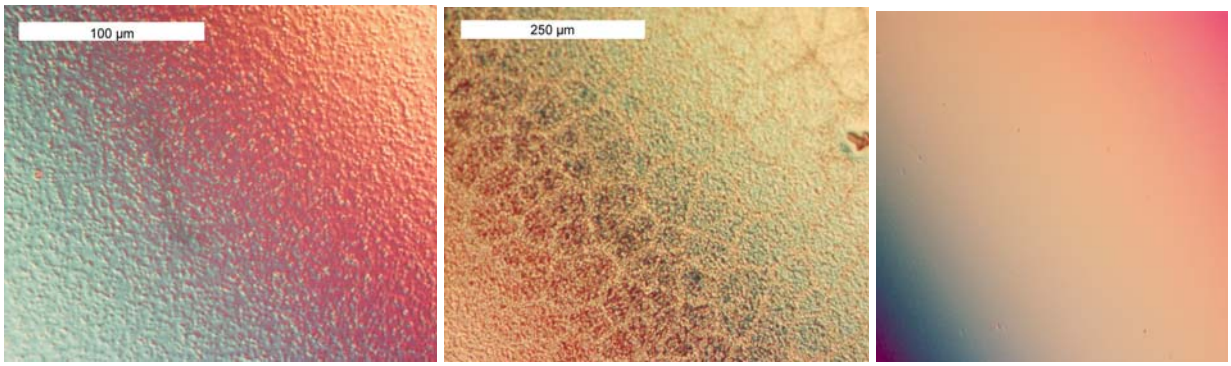

Figure 35. Precursor films with (a) bubbles, (b) Bénard cells and bubbles, and (c) no visible crystallization defects. The Nomarski filter was used to magnify or clarify the surface defects that could be formed at room temperature as well as after heat treatment.

4.3 Low Temperature Process

The solutions that were tested in the previous chapter were generally put through a single heat treatment, up to conversion temperatures, to obtain the final YBCO films. However, in order to obtain a high performance final film, the reactions that take place within that film must be understood so that an appropriate heat treatment could be applied. Problems such as cracking in

thicker films were already minimized by the solution design, but could be further prevented by tailoring the heat treatment. Various analytical techniques were used to determine the low temperature (<500ºC) reactions that took place in the precursor films as they were heat treated. The results of these analyses were compared to each other and, along with information found in the literature, used to construct the low temperature process. The low temperature process would produce stable intermediate films that could be analyzed for their thickness, any surface defects, and other factors such as presence of crystalline compounds such as barium nitrate, before they are put through the high temperature conversion process.

4.3.1 Low Temperature Reactions

4.3.1.1 Experimental Procedure

Thermogravimetric (TGA) and differential thermal analysis (DTA) were done using a Seiko Dual TG/DTA 320 Analyzer. The samples were heated up at a rate of 10ºC/min under a 150 cc/min flow of 100 ppm O_2/N_2 gas. XPS was done using a Kratos AXIS Ultra Imaging X-ray Photoelectron Spectrometer. FTIR analysis was done using a Nicolet Magna 860 Fourier Transform Infrared Spectrometer. XRD patterns were obtained using a Rigaku R-200 three-circle diffractometer with a rotating anode source at 50 kV and 300 mA.

4.3.1.2 Results and Discussion

The figure below shows the DTA analysis of a mixture of the nitrates and polymers that make up the precursor solution. This analysis was compared to that for a mixture of spray-dried nitrate powders, also shown below. The Y-nitrate decomposition peak was unclear and therefore unlabeled in the later figure, but according to the literature it was expected to be ~366ºC.

Comparison of these analyses showed that the presence of the polymers in the precursor resulted in a lowering of the decomposition temperatures of the nitrates, signified by the downward exothermic peaks. According to the literature, $Cu(NO_3)_2 \cdot 3H_2O$ decomposition took place by 256ºC, $Y(NO_3)_3 \cdot 5H_2O$ decomposition goes up to ~366ºC, and $Ba(NO_3)_2$ decomposed between 575ºC and 676ºC [61]. The interaction between the nitrates with each other [61] and between the nitrates and the organics [57,56] resulted in these decompositions taking place at lower temperatures. The combination of nitrates as oxidizing agents and the organics in the precursor resulted in conditions conducive to combustion in the precursor film during the decomposition heat treatment. The three exothermic peaks observed in the DTA of the polymer-nitrate mixture that signified the decomposition of the nitrates were shifted to lower temperatures than those cited by Lo et al and the DTA of the spray dried nitrates.

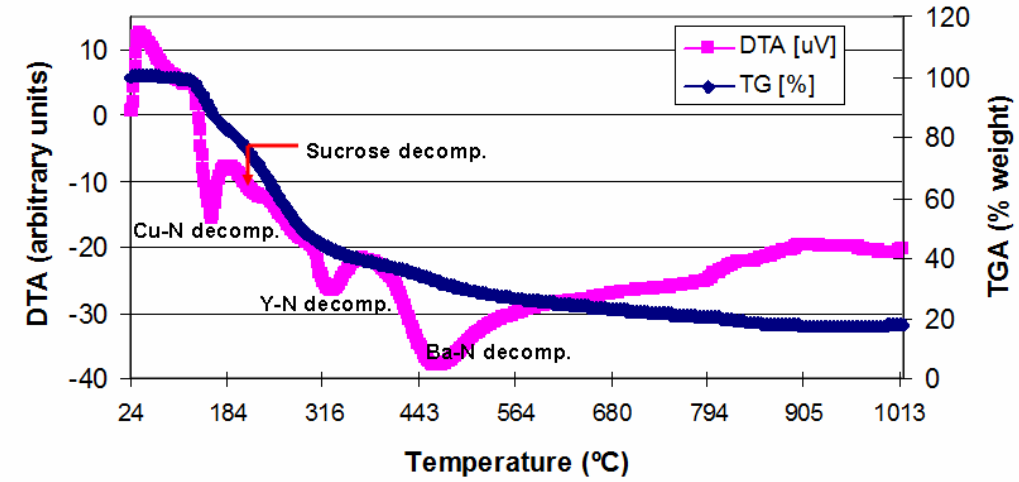

Figure 36. DTA and TGA analyses of precursor mixture of nitrates and polymers

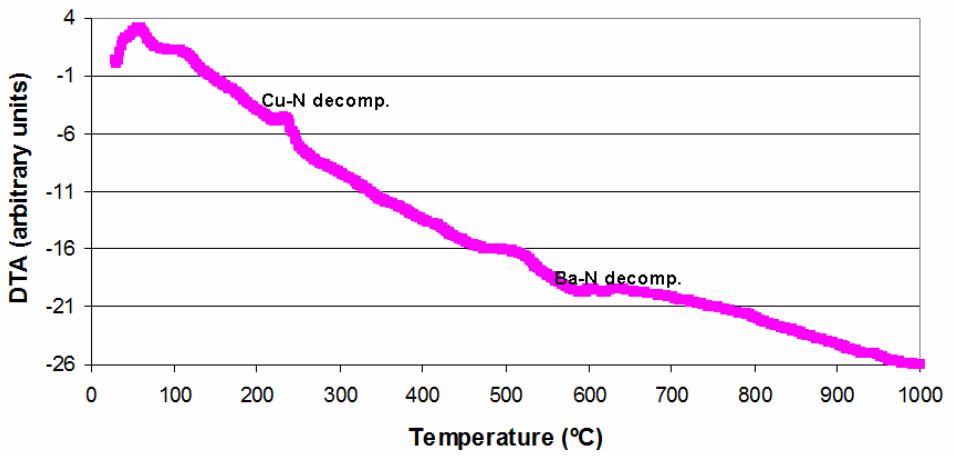

Figure 37. DTA analysis of spray-dried nitrate powders

The decomposition of sucrose in the precursor film led to a cross-linking caramelization reaction that produced a tougher film. The thermal decomposition of sucrose is a reaction taking place between 190ºC and 215ºC [54]. Hydrolysis of the sucrose in solution would also occur above 100ºC, producing fructose and glucose which have much lower decomposition temperatures (110ºC and 160ºC, respectively) [54]. A large amount, although not all, of the organic material was removed from the film upon this reaction. The TGA of the polymer-nitrate mixture showed a large weight loss during heating, including a significant weight loss (~60 wt %) up to approximately 300ºC. This weight loss took place as a result of the decomposition of substantial amounts of the nitrates and polymers in the precursor, and the subsequent removal of nitrates and carbon from the film. This was supported by FTIR and XPS data, presented in the figures below. The FTIR data showed nitrogen coming out of the film in the form of N_2O at approximately 125ºC. The nitrogen came off the film as NO_x gas beyond that temperature, but NO_x signals were more difficult to detect than the N_2O signal. XPS data, however, supported the claim that nitrogen was removed from the film at low temperatures; nitrogen was detected in the film at lower temperatures but not beyond 400ºC. It is noted that the FTIR data and XPS data are

for PVA-nitrate films. Spin-coated green HEC-nitrate precursor films were unstable in air, and would therefore not give an accurate picture of what was happening in the film as it was heat treated. However, the information gained from the FTIR and XPS data of quenched PVA-nitrate films could still be applied to the understanding of the reactions in polymer-nitrate films in general.

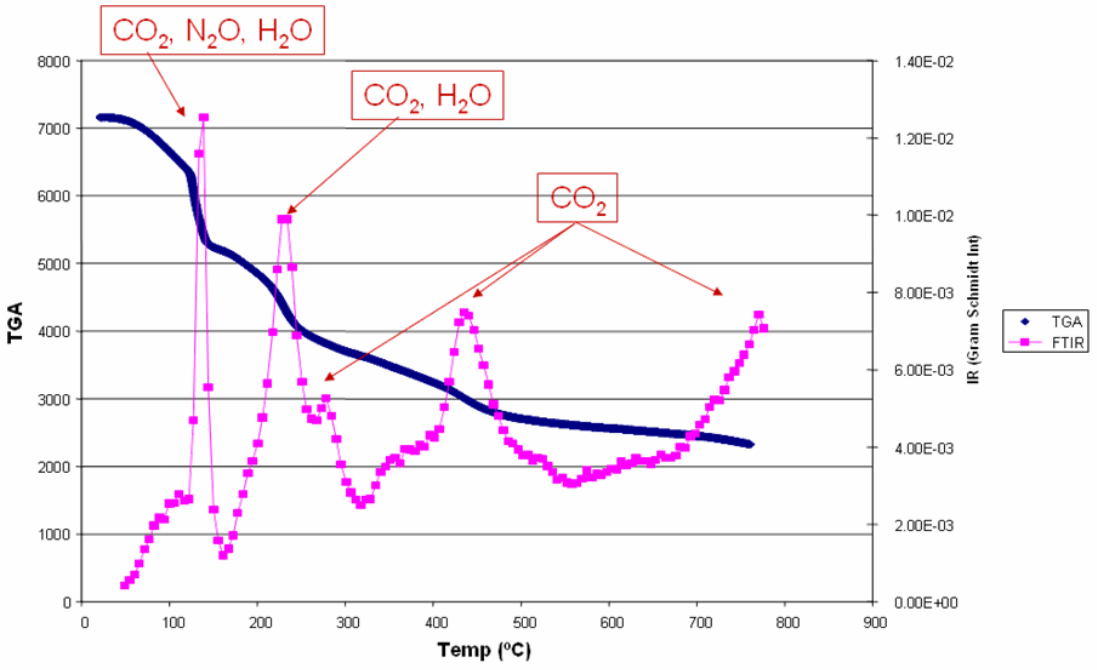

Figure 38. FTIR data for PVA-nitrate film, showing gas evolution during heat treatment

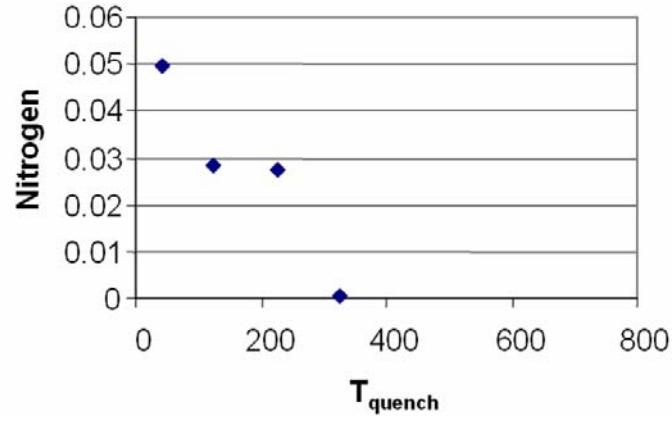

Figure 39. XPS data showing nitrogen signal disappearing under 400°C

The various reactions taking place at low temperatures suggested that a low temperature heat treatment to obtain an intermediate, decomposed, film may be used for this non-fluorine system. The thermal decomposition of sucrose, expressed as an exothermic signal beginning at 190ºC and with a peak at 215ºC, resulted in a cross-linking reaction that produced a tougher film. High amounts of sucrose in the precursor solution had been shown to produce defects on the film surface due to the surface tension that resulted from this cross-linking reaction. However, the reduced total chelator content in the final precursor solution in addition to the fast post-spin coating drying process prevented these defects from forming on the surface. Cross-linking still took place in the film, evidenced by the decomposition peak slightly visible in the DTA curve of the nitrate-polymer mixture. A film processed to a temperature after this decomposition event would be stable under ambient atmosphere, and could be processed in preparation for the high temperature conversion heat treatment.

4.3.2 Low-T Decomposition Heat Treatment

Based on the analyses discussed in the previous sub-section, a low temperature process was developed as an intermediate decomposition step for the precursor films. The green films were heated at a ramp rate of 5ºC/min to 275ºC under flowing 100 ppm O_2/N_2 atmosphere, and then quench-cooling the samples once they reach 275ºC.

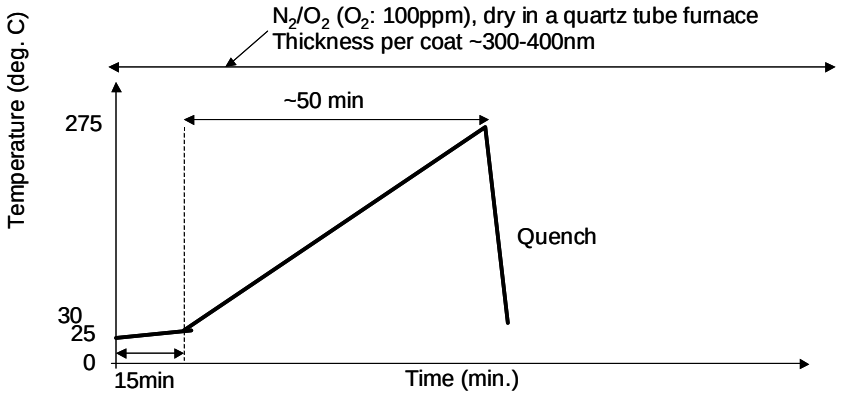

Figure 40. Low-temperature decomposition heat treatment process

Current paths were scribed on the decomposed films, their thicknesses were measured using a Tencor P10 profilometer, and other sample data were taken, including optical micrographs and XRD. The thickness of decomposed films ranged from 2 to 3 microns and the films were smooth, with RMS roughness of less than 1% of the film thickness. A typical XRD pattern taken of a decomposed film, presented below, showed that the crystalline peaks corresponded only with the LAO substrate. A wide peak was also detected, suggesting the presence of amorphous mixtures of the precursor ingredients. The decomposed films contained mixtures of oxides and carbon [36]. Any remaining nitrates would decompose by ~400ºC, leaving the oxide and carbon mixture in the film. This film state was similar to the state of intermediate films formed by other groups working on other high-performance non-fluorine solution deposition processes, such as the acetylacetonate process [19].

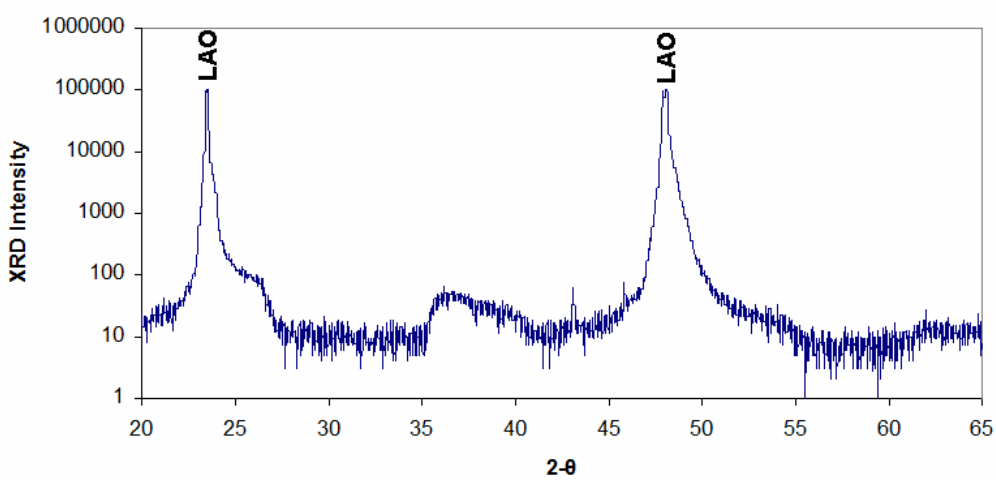

Figure 41. XRD of decomposed film

4.4 Conversion to YBCO

Decomposed films that were free of surface defects and had the desirable green thickness (~2.3-2.5 μm) were put through a high temperature conversion heat treatment also developed at MIT [36]. This conversion heat treatment was done at a ramp rate of ~15ºC/min. Hold segments could be inserted at different temperatures, usually between 500ºC and 700ºC, for 15 minutes to several hours, before continuing to the annealing temperature. The conversion heat treatment was generally done under 100 ppm O_2/N_2, but different atmospheres could be used at different temperatures to control the various reactions, including carbon removal and YBCO nucleation and growth. These may include UHP N_2, 1000 ppm O_2, and UHP O_2. Pure O_2 gas was flown over the films at some point during cool-down to room temperature. A separate O_2 annealing step for one hour at 450ºC was also applied to the converted films.

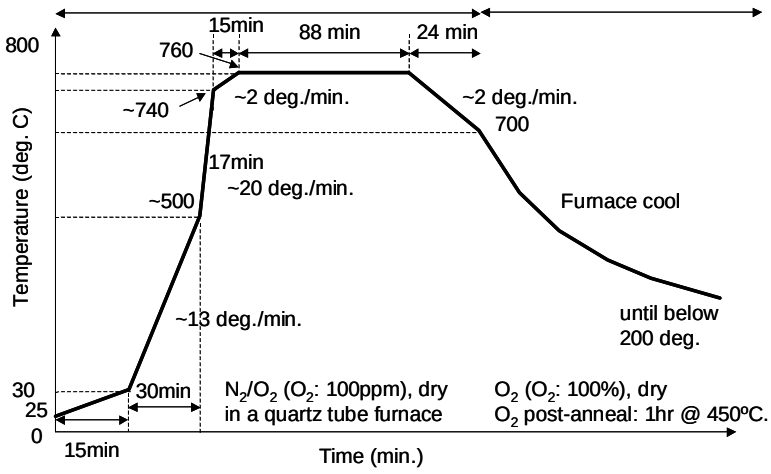

Figure 42. High temperature conversion heat treatment profile

The resulting YBCO films were c-axis textured, with clear (001) peaks visible in XRD, and carried current with critical currents up to nearly 60 A/cm. J_c values of over 1 MA/cm^2 were reproduced for films with final thicknesses that could exceed 400 nm. This was a vast improvement over the MA/cm^2 films made from the other polymer-nitrate (mainly PVA-nitrate) solutions discussed in Chapter 2 that were only about 150 nm thick. Some second phases were observed both in XRD and in SEM micrographs. AES analysis suggested these second phases to be mainly barium and copper rich second phases, which were detected as barium cuprate in XRD, as well as some copper oxide second phases, which were not detected in XRD. A typical XRD pattern for a high-performance YBCO film is presented below, along with an SEM of a YBCO film with an I_c of 57.7 A/cm.

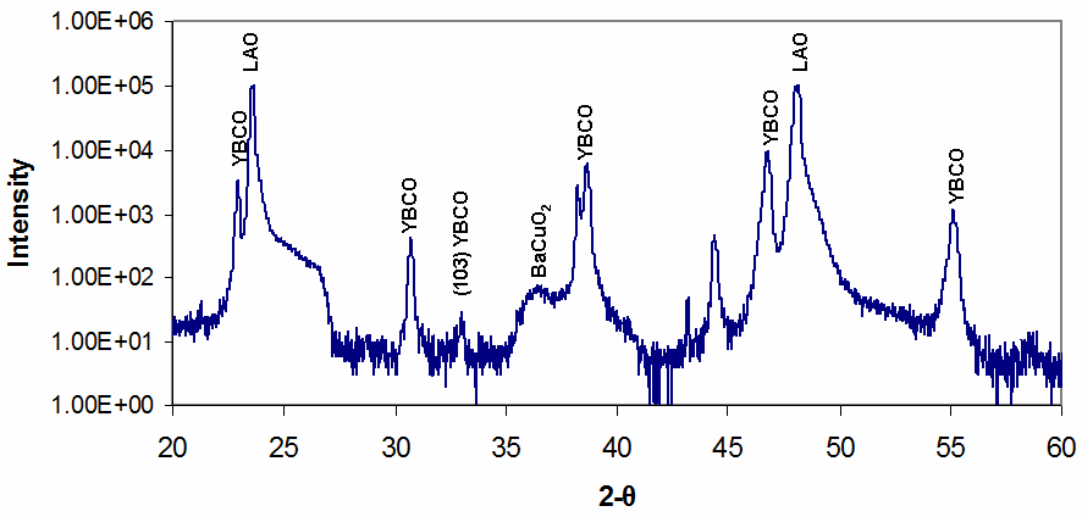

Figure 43. Typical XRD of YBCO film made from non-fluorine process

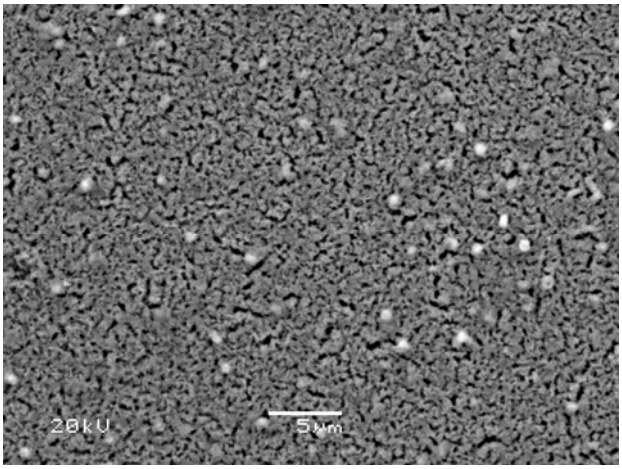

Figure 44. YBCO film with I_c = 57.7 A/cm

4.5 Summary

Analytical techniques such as DT/TGA, FTIR, and XPS were used to determine the reactions that would take place during heat treatment. A low temperature decomposition process was developed based on these analyses. The process was used to obtain smooth, defect free intermediate films that could be further heat treated to form high performance YBCO films.

CHAPTER 5: SUMMARY AND FUTURE WORK

A non-fluorine precursor solution system for producing MA/cm^2 YBCO films was developed. This thesis work encompassed the selection of a non-fluorine precursor solution from three possible solution systems, the development of that precursor solution, and the production of high performance YBCO films using the completed precursor solution. The three solution systems that were tested included the trimethylacetate (TMA) solution system, the alkoxide-particle solution system, and the polymer-nitrate solution system.

The polymer-nitrate precursor solution was selected for several reasons. It did not involve an intermediate chemical reaction step prior to mixing the three cations together, and therefore ensured a straightforward and reproducible way of maintaining the desired cation stoichiometry. The polymer-nitrate precursor solution also had flexibility in the incorporation of different polymers; several polymers were tried and the resulting precursor solutions were used to produce YBCO films with J_c values of at least 0.5 MA/cm^2. The polymer-nitrate precursor solution was stable at room temperature with the exception of the barium nitrate, but that did not prevent the spin-coating of smooth, uniform green films. Aliquots of the solution simply had to be heated to ~80ºC immediately preceding spin-coating. This was a stark contrast with the alkoxide-particle precursor solution, which experienced sedimentation of remaining or newly-formed copper oxide agglomerates from the suspension, despite the presence of a dispersant. The TMA and alkoxide-particle solutions both had low total cation concentrations; the polymer-nitrate solution allowed for higher cation concentrations, thus leading to higher final film thicknesses and densities. Finally, the use of water as a solvent was far preferable than the hydrolysable alkoxides or the toxic propionic acid/amylamine solvent in the TMA precursor solution.

The selected polymer-nitrate solution had many challenges that needed to be addressed, including low initial total cation concentration, cracking in thicker films, overall thickness limitations, barium nitrate crystallization, and film delamination. These challenges were each addressed by modification of the specific contents of the precursor solution. Chelating agents were adopted to prevent barium nitrate crystallization. A small vacuum apparatus was used alongside a nitrogen glovebox to produce spin-coated films that were crystallization free and stable enough to be placed in the tube furnace for further processing. HEC was selected as a rheology modifier for its effectiveness in increasing the viscosity of the precursor solution, thereby increasing the deposited film thickness. A hot-solution method was also adopted, allowing for higher cation concentrations with minimal amount of organics in the precursor film. This increased the final film thickness up to nearly one micron for a single deposited layer, and prevented problems associated with high organic contents, including cracking and film delamination. Delamination was fixed by the combination of low organic content, HEC as a rheology modifier, and PEG doubling as a chelating agent and as a plasticizer. The final non-fluorine precursor solution was an HEC-nitrate-PEG-sucrose solution with a cation ratio of Y: Ba: Cu = 1: 2: 3.

The HEC-nitrate precursor solution was used to produce films with > 1 MA/cm^2 critical current densities and thicknesses over 400 nm. c-axis (001) textured YBCO was detected in XRD, along with barium cuprate second phases. Thermal analyses were done to determine that decomposition of nitrates and organics took place in the films before 400ºC, and that the nitrogen was no longer detected by XPS at temperatures above 400ºC. An intermediate decomposition heat treatment was developed based on the thermal analyses of the reactions taking place in the precursor film as it was heated up. This intermediate decomposition step yielded smooth,

uniform, surface defect-free, robust films that could be scribed before being placed back in the furnaces for the high temperature conversion to YBCO. However, intermediate films thicker than ~2.5 μm still tended to have surface defects. Additional in-depth thermal analysis (including DSC, higher resolution DT/TGA) would further show how these defects develop, and adjustments to the decomposition process could be made accordingly. This in-depth thermal analysis could illuminate additional thermal reaction peaks that were not quite detected in the thermal analyses done here.

An in-depth study of the microstructural evolution of the precursor film by cross-sectional and high-resolution plan-view TEM is of interest. This microstructural evolution can be compared with those for other processes that have produced higher performance coated conductors of higher thicknesses. These comparisons will be very helpful in directing further ways of improving the performance of YBCO films obtained from this polymer-nitrate precursor solution.

REFERENCES

1. Larbalestier, D., A. Gurevich, D.M. Feldmann, and A. Polyanskii: High-T_c superconducting materials for electric power applications. *Nature*, 414, 368-377 (2001).
2. Paranthaman, M. P., and T. Izumi: High-performance YBCO-coated superconductor wires. *MRS Bulletin*, 533-541 (2004).
3. Araki, T., et al: High-J_c $YBa_2Cu_3O_{7-x}$ films on metal tapes by the metalorganic deposition method using trifluoroacetates. *Supercond. Sci. Technol.*, 15, L1-L3 (2002).
4. Araki, T. and I. Hirabayashi: Review of a chemical approach to $YBa_2Cu_3O_{7-x}$-coated superconductors—metalorganic deposition using trifluoroacetates. *Supercond. Sci. Technol.*, 16, R71-R94 (2003).
5. Hawsey, R. A.: Overview of U.S. Department of Energy Superconductivity Program for Electric Power. *Mat. Res. Soc. Symp. Proc.*, 689, E6.1.1-10 (2002).
6. Yurek, G.: HTS Industry Status and Outlook. DOE Superconductivity for Electric Systems 2005 Annual Peer Review, Washington, D.C., http://www.amsuper.com (2005).
7. Masur, L.J., et al: The status of commercial and developmental HTS wires. *Physica C.*, 392-396, 989-997 (2003).
8. Coated conductor technology development roadmap: US Department of Energy Superconductivity for Electric Systems Program, *http://www.ornl.gov/sci/htsc/documents/pdf/CCRoadmap8-23.pdf* (2001).
9. Iijima, Y., N. Tanabe, O. Kohno, and Y. Ikeno: In-plane aligned $YBa_2Cu_3O_{7-x}$ thin films deposited on polycrystalline metallic substrates. *Appl. Phys. Lett.*, 60 (6), 769-771 (1992).
10. Iijima, Y., N. Tanabe, O. Kohno, and Y. Ikeno: In-plane aligned $YBa_2Cu_3O_{7-x}$ thin films deposited on polycrystalline metallic substrates. *Appl. Phys. Lett.*, 60 (6), 769-771 (1992).
11. Goyal, A., et al: High critical current density superconducting tapes by epitaxial deposition of $YBa_2Cu_3O_x$ thick films on biaxially textured metals. *Appl. Phys. Lett.*, 69 (12), 1795-1797 (1996).
12. Feldmann, D.M., et al: Grain orientations and grain boundary networks of $YBa_2Cu_3O_{7-\delta}$ films deposited by metalorganic and pulsed laser deposition on biaxially textured Ni-W substrates. *J. Mater. Res.*, 21 (4), 923-934 (2006).
13. Dimos, D. and P. Chaudhari: Superconducting transport properties of grain boundaries in $YBa_2Cu_3O_7$ bicrystals. *Phys. Rev. B*, 41 (7), 4038-4050 (1990).
14. Dimos, D., P. Chaudhari, J. Mannhart, and F. K. LeGoues: Orientation dependence of grain-boundary critical currents in $YBa_2Cu_3O_{7-\delta}$ bicrystals. *Phys. Rev. Lett.*, 61 (2), 219-224 (1988).
15. Larbalestier, D., R.D. Blaugher, R. E. Schwall, R. S. Sokolowski, M. Suenaga, J. O. Willis: Power applications of superconductivity in Germany and Japan. World Technology Evaluation Center (WTEC) (1997). *http://www.wtec.org/loyola/scpa/toc.htm*
16. Foltyn, S.R., et al: Overcoming the barrier to 1000 A/cm width superconducting coatings. *Appl. Phys. Lett.*, 87, 162505 (2005).
17. Holesinger, T. and L. Civale: Multi-scale characterization: evaluation of microstructural and superconducting properties across multiple length scales in 2nd generation HTS wire. *2006 DOE Superconductivity Program Peer Review*, July 25-27 (2006).
18. Bhuiyan, M.S., M. Paranthaman, and K. Salama: Solution-derived textured oxide thin films—a review. *Supercond. Sci. Technol.*, 19, R1-R21 (2006).

19. Tsukada, K., M. Furuse, M. Sohma, T. Manabe, I. Yamaguchi, W. Kondo, S. Fuchino, T. Kumagai: Preparation of high-J_c $YBa_2Cu_3O_{7-y}$ films on CeO_2-buffered yttria-stabilized zirconia substrates by fluorine-free metalorganic deposition. *Jpn. J. App. Phys.*, **44 (7A),** 4914-4918 (2005).
20. F. Lu and E.E. Hellstrom: Deposition of $SmBa_2Cu_3O_{7-d}$ films on RABiTS templates by a fluorine-free MOD process. 5MI03 Poster presented at Applied Superconductivity Conference, Seattle, WA 2006.
21. Apetrii, C., H. Schlorb, M. Falter, I. Lampe, L. Schultz, D. Holzapfel: YBCO thin films prepared by fluorine-free polymer-based chemical solution deposition. IEEE Trans. Appl. Supercond., 15, 2642-2644 (2005).
22. Smith, J.A., M.J. Cima, and N. Sonnenberg: High critical current density thick MOD-derived YBCO films. *IEEE Trans. Appl. Supercond.*, 9 (2), 1531-1534 (1999).
23. McIntyre, P.C., et al: Effect of growth conditions on the properties and morphology of chemically derived epitaxial thin films of $Ba_2YCu_3O_{7-x}$ on (001) $LaAlO_3$. *J. Appl. Phys.*, 71 (4), 1868-1877 (1992).
24. Batson, P.E., T.M. Shaw, D. Dimos, and P. R. Duncombe: Participation of carbon in the electronic structure of $YBa_2Cu_3O_{7-\delta}$. *Phys. Rev. B*, 43 (7), 6236-6238 (1991).
25. Shaw, T.M., et al: Carbon retention in $YBa_2Cu_3O_{7-\delta}$ and its effect on the superconducting transition. *J. Mater. Res.*, 5 (6), 1176-1184 (1990).
26. Yoshizumi, M., I. Seleznev, and M.J. Cima: Reactions of oxyfluoride precursors for the preparation of barium yttrium cuprate films. *Physica C*, 403, 191-199 (2004).
27. Hamdi, A.H., et al: Formation of thin-film high T_c superconductors by metalorganic deposition. *Appl. Phys. Lett.*, 51 (25), 2152-2154 (1987).
28. Kumagai, T., et al: Preparation of high J_c $Ba_2YCu_3O_{7-\gamma}$-Ag composite films on $SrTiO_3$ (100) substrates by the dipping-pyrolysis process. *Appl. Phys. Lett.*, 61 (8), 988-990 (1992).
29. Li, X-G., M-R. Huang, H. Bai: Thermal decomposition of cellulose ethers. *J. Appl. Pol. Sci.*, 73, 2927-2936 (1999).
30. Shi, D., Y. Xu, H. Yao, J. Lian, L. Wang, A. Li, and S.X. Dou: The development of $YBa_2Cu_3O_x$ thin films using a fluorine-free sol-gel approach for coated conductors. *Supercond. Sci. Technol*. **17** 1420-1425 (2004).
31. Gupta, A., G. Koren, E.A. Giess, N.R. Moore, E.J.M. O'Sullivan, E.I. Cooper: $Y_1Ba_2Cu_3O_{7-\delta}$ thin films grown by a simple spray deposition technique. *Appl. Phys. Lett.*, 52 (2), 163-165 (1988).
32. Xu, Y., A. Goyal, J. Lian, A. Rutter, S. Shi, S. Sathymurthy, M. Paranthaman, L. Wang, P.M. Martin, and D.M. Kroeger: Preparation of YBCO films on CeO_2-buffered (001) YSZ substrates by a non-fluorine MOD method. *J. Am. Ceram. Soc.* **87** [9] 1669-1676 (2004).
33. Xu, Y., A. Goyal, K. Leonard, and P. Martin: High performance YBCO films by the hybrid of non-fluorine yttrium and copper salts with Ba-TFA. *Physica C*, **421**, 67-72 (2005).
34. Mukhopadhyay, S.M. et al: Performance enhancement of second generation coated conductors by investigation of flux pinning and AC loss issues. *2005 DOE Peer Review in Washington DC,* (2005).
35. Wesolowski, D.E., and Cima, M.J.: Nitrate-based metalorganic deposition of CeO_2 on yttrium-stabilized zirconium. J. Mater. Res., Vol. 21, No. 1, January 2006.

36. Wesolowski, D.E: Conversion of Solution-Deposited YBCO Coated Conductors. Doctoral Thesis, Massachusetts Institute of Technology, June 2008.
37. Supardi, Z., Supardi, G. Delabouglise, C. Peroz, A. Sin, C. Villard, P. Odier, F. Weiss: Epitaxial thick film of YBCO by high temperature spray pyrolysis for coated conductors. *Physica C*, 386, 296-299 (2003).
38. Ng, M.F and M.J.Cima: Heteroepitaxial growth of lanthanum aluminate films derived from mixed metal nitrates. *J. Mater. Res.*, 12, 1306-1314 (1997).
39. Stewart, E., M.S. Bhuiyan, S. Sathyamurthy, and M. Paranthaman: Studies of solution deposited cerium oxide thin films on textured Ni-alloy substrates for YBCO superconductor. *Materials Research Bulletin* 41 1063–1068 (2006).
40. Wang, S.S., Z. Han, H. Schmidt, H. W. Neumuller, P. Du, L. Wang, and S. Chen: Chemical solution growth of CeO_2 buffer and YBCO layers on IBAD-YSZ/Hastelloy templates. *Supercond. Sci. Technol.,* 18, 1468-1472 (2005).
41. Jia, Q., T.M. McCleskey, A.K. Burrell, Y. Lin: Polymer-assisted deposition of films. *United States Patent Application* 20050043184 (2005).
42. Rice, C.E., R.B. van Dover, and G.L. Fisanick: Preparation of superconducting thin films of $Ba_2YCu_3O_7$ by a novel spin on pyrolysis technique. *Appl. Phys. Lett* **51** [22] 1842 (1987).
43. Kordas, G.: Sol-gel processing of ceramic superconductors. *J. Non-Crys. Sol.,* **121**, 436-442 (1990).
44. Bowmer, T. N. and F. K. Shokoohi: Synthesis of superconductors from metal neodecanoates. *J. Mater. Res.,* **6**, 670-675 (1991).
45. Chu, P.-Y. I. Campion, and R. C. Buchanan: Processing effects on high T_c properties of $YBa_2Cu_3O_{7-x}$ films from carboxylate solution precursors. *J. Mater. Res.*, 8[2], 261-267 (1993).
46. Schoop, U., M. W. Rupich, C. Thieme, D. T. Verebelyi, W. Zhang, X. Li, T. Kodenkandath, N. Nguyen, E. Siegal, L. Civale, T. Holesinger, B. Maiorov, A. Goyal, and M. Paranthaman: Second Generation HTS wire based on RABiTS substrates and MOD YBCO. *IEEE Trans. App. Supercond.,* 15 (2), 2611-2616 (2005).
47. Dean, J.A..: Solubilities of inorganic compounds and metal salts of organic acids in water at various temperatures. *Lange's Handbook of Chemistry (15th Edition)*, McGraw-Hill, (1999).
48. Rogers, R.D., M.L. Jezl, and C.B. Bauer: Effects of polyethylene glycol on the coordination sphere of strontium in $SrCl_2$ and $Sr(NO_3)_2$ complexes. *Inorg. Chem.*, 33, 5682-5692, (1994).
49. Reed, J.S. *Principles of Ceramics Processing*. 1995. New York: John Wiley and Sons.
50. Sakellariou, P. et al: The interactions and partitioning of low molecular weight polyethylene glycols and diethyl phthalate in ethylcellulose / hydroxypropyl methylcellulose blends. *J. Appl. Pol. Sci.*, 34, 2507-2516, (1987).
51. Marrion, A.R.,ed. *The Chemistry and Physics of Coatings*. 2004. Cambridge: The Royal Society of Chemistry.
52. Yang, L., et al: Interactions between metal ions and carbohydrates: coordination behavior of neutral erythritol to Ca(II) and lanthanide ions. *Inorg. Chem.*, 42, 5844-5856, (2003).
53. Erkselius, S. and O.J. Karlsson: Free radical degradation of hydroxyethyl cellulose. *Carbohydrate Polymers*, 62, 344-356 (2005).

54. Harwalker, V.R. and C-Y. Ma, eds. *Thermal Analysis of Food*. Elsevier Science Publishers, Ltd. (1990).
55. Bates, F., F.P. Phelps, and C.F. Snyder: Saccharimetry, the properties of commercial sugars and their solutions. *International Critical Tables*.
56. Lampe, I.v., D. Schultze, F. Zygalsky, M.S. Silverstein: Thermal degradation of Y–Ba–Cu and Bi–Sr–Ca–Cu precursors for the preparation of high temperature superconductors. *Polymer Degradation and Stability* 81, 57–63 (2003).
57. Kourtakis, K. M. Robbins, and P. K. Gallagher: A Novel Synthetic Method for the Preparation of Oxide Superconductors: Anionic Oxidation-Reduction. *J. Sol. State Chem*. 82, 290-297 (1989).
58. Araki, T., et al: Growth model and the effect of CuO nanocrystallites on the properties of chemically derived epitaxial thin films of $YBa_2Cu_3O_{7-x}$. J. Appl. Phys., 92 (6), 3318-3325 (2002).
59. Dubinsky, S., et al: Thermal degradation of poly(acrylic acid) containing metal nitrates and the formation of $YBa_2Cu_3O_{7-x}$. *J. Pol. Sci. Part B*, 43, 1168-1176 (2005).
60. Goto, T. and I. Horiba. A method for producing high-T_c Y-Ba-Cu-O superconducting filaments by die-free spinning. *Japanese Jour. Appl. Phys.*, 26 (12), L-1970-L-1972 (1987).
61. Lo, W., et al: Preparation and properties of spray dried precursor powder for melt-processed bulk YBCO ceramics. *J. Mater. Res.*, 11 (1), 39-49 (1996).
62. Lumelsky, Y., and M.S. Silverstein: The degradation of novolak containing metal nitrates and the formation of YBCO. *J. Mater. Sci.* 41, 8202-8210 (2006).
63. Malozemoff, A.P., et al: Low-cost YBCO coated conductor technology. *Supercond. Sci. Technol.,* 13, 473-476 (2000).
64. Schoff, C.K.: Concentration dependence of the viscosity of dilute polymer solutions: Huggins and Schulz-Blaschke constants. *Knovel Engineering and Scientific Handbooks*, (2005).
65. Tang, X., B.Y. Zhao, and K.A. Hu: Preparation of M-Ba-ferrite fine powders by sugar-nitrates process. *J. Mater. Sci.*, 41, 3867-3871, (2006).
66. Wypych, G. Plasticizers use and selection for specific polymers. ChemTec Laboratories, Inc., Publishing, Toronto, Canada (2001).